



www.maajournal.com

*Mediterranean Archaeology and Archaeometry*  
Vol. 23, No 1, (2023), pp. 93-133  
Open Access. Online & Print.



DOI: 10.5281/zenodo.7604969

# RECONNAISSANCE ARCHAEOLOGY OF JABAL DHAYLAN, RED SEA, SAUDI ARABIA

Charles G. Clifton

*Geological Society of Nevada, USA*  
([gcliftongeo@gmail.com](mailto:gcliftongeo@gmail.com))

Received: 18/12/2022

Accepted: 19/01/2023

---

## ABSTRACT

Jabal Dhaylan is a small, isolated mountain on the coastal plain of the Red Sea surrounded by tens of kilometers of featureless sand. The mountain is composed of granitic rocks that were partially covered by limestone reefs during the opening of the Red Sea. The limestone is locally mineralized with deposits of high grade zinc that have attracted geologists since 1968. In the course of evaluating the deposits in 2005-2006, the author encountered many archaeological features, including petroglyphs containing tribal symbols (wusum), rock art depicting animal and human forms, burial cairns, and grinding stones. The finds also include a Paleolithic rock quarry with Levallois style cores, and evidence of silver smelting dating back to 3800 BC, based on dates obtained on a fragment of crucible (cupule) by thermoluminescence. A second period of mining that correlates with the expansion of the Arab empire in the late 7th century was identified from fragments of charcoal, which returned Carbon-14 dates of 692, 670, and 633 AD. It was determined that silver was not found at the mining location; it is probable that galena and calamine were extracted as trade items, possibly for medicinal applications. The tribal symbols were found to be the same symbols used by the Bedouins living in the area today. Family members who left the local clan in the distant past were traced to southern Spain, based on tribal symbols found on a stone stela near Cordoba. Historic accounts suggest this family entered Spain as part of the Arab conquest in 712 AD and settled there. The purpose of this report is to record what was observed for the archaeological record, and to connect these observations to present-day people and historical facts where possible. This paper describes what was found in the course of geologic work at Jabal Dhaylan; an exhaustive survey of archaeological sites was not undertaken and additional features are likely to be present.

---

**KEYWORDS:** Petroglyphs, Wusum, Cairns, Bedrock Mortars, Silver, Calamine, Galena, Kohl, Levallois, al Andalus

---

## 1. INTRODUCTION

This report describes archaeological features that were observed in 2005-2006 while the author was employed as a geologist to evaluate zinc deposits in the area of Jabal Dhaylan, a small, isolated mountain on the Red Sea in western Saudi Arabia. The location is remote and only one small source of surface water is present. There is no evidence the area once supported a permanent population. Most of the archaeological features can be attributed to Bedouins who passed through the area or lived in scattered camps and depended on camels for subsistence. There are no substantial archaeological sites nearby, the nearest being at Umm Lajj to the south and al Wajh to the north. Because of its remote location, the archaeological features at Jabal Dhaylan appear to be associated with a single Bedouin clan that has inhabited the area since pre-Islamic time, an observation that is the central focus of this report. An effort has been made to describe all of the archaeological features in the area, including petroglyphs with tribal symbols (wusum), depictions of animal and human forms (rock art), the purpose of ancient mining at one location, and a stone quarry of possible Paleolithic age.

## 2. LOCATION AND GEOLOGY

Jabal Dhaylan is located on the coastal plain of the Red Sea, 425 km north of Jeddah, 50 km north of Umm Lajj, and 105 km south of Al Wajh (Fig. 1). The mountain is 3 km north of the highway at the Jabal al Uqqar service station on the coastal highway linking Jeddah and the border with Jordan (Fig. 2). The coast of the Red Sea is 12 km to the west and the escarpment marking the Arabian Shield is 10 km to the east. The area is desolate with a few acacia trees and scattered acacia shrub. A single source of surface water is located on the west side of the mountain. There is no known mention of archaeological sites at Jabal Dhaylan in the scientific literature or government reports. Bedouin camps are present north and south of the highway. The location is known for small but rich zinc deposits that were emplaced in Miocene age reef limestones that covered a shallow, partially submerged island of Precambrian age granite during the opening of the Red Sea. The granitic rocks are part of the Arabian Shield that continues beneath the Red Sea

to the northern coast of Egypt and Sudan. The zinc deposits were discovered by French geologists of the Bureau de Recherche Géologiques et Minières (BGRM) in 1968-1972 in a mineral survey for the Saudi Arabian Deputy Ministry for Mineral Resources (DMMR). The area was further evaluated by the United States Geological Survey in 1996-2000 (Hayes et al., 2001, 2002), and again in 2005-2006 by Petro-Hunt Middleeast Company. The writer was the project geologist for Petro-Hunt and archaeological observations were made in the course of managing the drilling program and conducting geologic mapping. Each of the archaeological features discussed below was visited for just a few minutes. Photos were taken, GPS locations recorded, and mental notes were made of what appeared to be important. Some of the photos were later discussed with the Sheikh of the local Bedouin clan, who made important observations that made much of this report possible. The archaeological features scattered around the mountain can be grouped into three locations, here designated Areas A, B, and C. Each area will be discussed in turn.



Figure 1. Jabal Dhaylan is located just north of the highway linking Jeddah with the Jordanian border. It is 425 km north of Jeddah, 200 km north of Yanbu and 105 km south of Al Wajh.

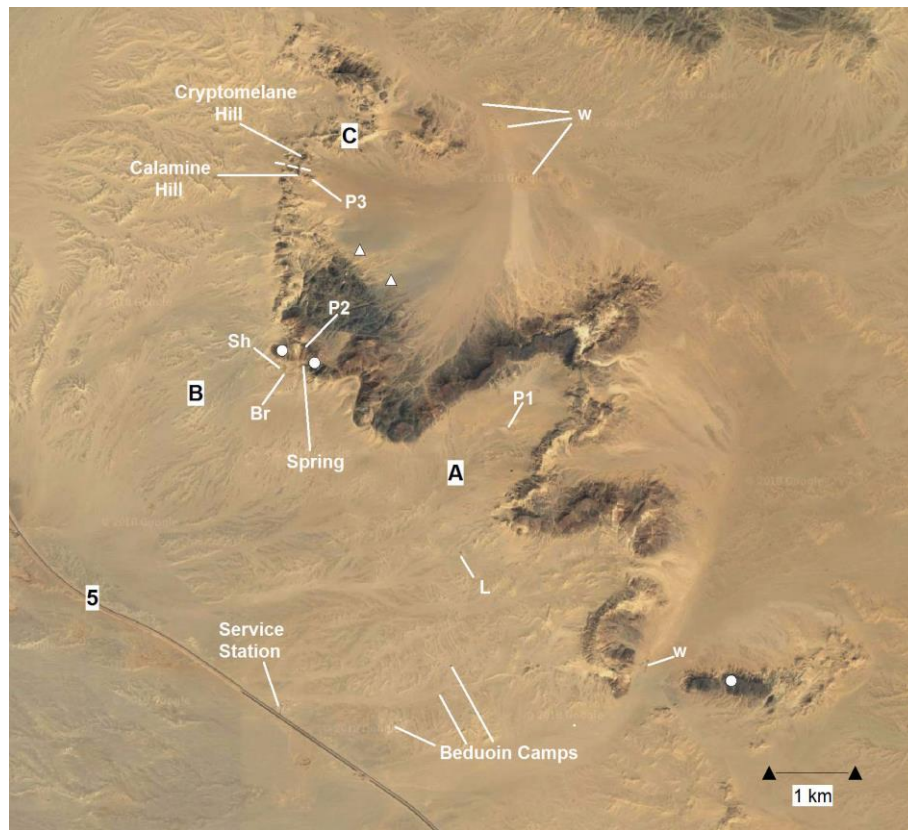


Figure 2. Jabal Dhaylan is approximately 3 km north of Highway 5 at the service station. P (petroglyphs), L (lithic site), Sh (terracotta shards), Br (bedrock mortars), w (walled camps with wells), solid circles (burial cairns, highlands), solid triangles (burial cairns, flats). A, B, C (areas discussed in text). Google Earth image.

## 2.1 The Bedouin Clan

Much of this report revolves around the history of the local Bedouin clan. The identities of the individual families and their tribal symbols are provided for the historical record. As the country becomes more prosperous, fewer Bedouins are keeping camels and their tribal symbols may be forgotten with time. At least one family in the clan has been sedentary for 50-60 years and long ago stopped keeping camels. The Bedouin families that live in scattered camps at Jabal Dhaylan belong to the al Jehani (Jahani) clan, a member of the Juhayna tribe that is centered around the cities of Medina, Yanbu, Umm Lajj, and Tabuk. The lands of the Juhayna were granted to the tribe by the Prophet Muhammad in 624 and stretch from Yanbu to the Gulf of Aqaba (MacMichael, 1922). The Juhayna tribe is mentioned throughout Arab history. It is the largest tribe of the Banu Quda'a, a confederation of Arab tribes that date from the 4th century or earlier (Smith et al., 1996, p. 94; Blankinship, 1994, p. 54). The Quda'a are mostly nomadic and are located primarily in northwest Arabia and Syria. Jehani is a derivative of the name Juhayna or Juhaynah. The antiquity of the name al Jehani is evidenced in historical figures that date to the time of the Prophet Muhammad, such as the Islamic scholar Ma'bad ibn Kalid al-Juhani, who died in 699 CE, and Abdallah bin Unays al-Juhani, a

companion to the Prophet Muhammad and military general who died in 674 CE. At Jabal Dhaylan, the al Jehani clan comprises 4 or 5 families, totaling 50-75 persons, mostly children. These include the family of Sheikh Abdullah al Jehani, in 2006 a young man of 27 who accompanied me during field work and was instrumental in identifying the tribal symbols that were discovered in the area. The Sheikh lived in a compound of permanent cement structures located one kilometer east of the service station. Evidence suggests his family had been sedentary since his birth. Abdullah's uncle, Salman al Jehani, lived nearby and kept several camels for milk. The family of Masaid Awada al Jehani lived in a tent camp south of Highway 5, and the family of Hamad Fiede al Jehani lived in a wadi a kilometer north of the service station. Masaid and Hamad are cousins and both kept camels. Hamad kept most of his camels at the town of Umm Lajj 50 kilometers to the south, but several were spotted in a larger herd kept by Masaid. Hamad reportedly walked his camels to a location near Yanbu each year.

## 3. SAMPLES AND METHODS

Materials from a site of ancient mining in Area C were collected for geochemical analysis and dating. These included 8-10 small (1.5 cm square) pieces of

charcoal and a single fragment of crucible (cupule) approximately 7 x 5 cm in size.

### 3.1 Elemental Analysis

A fragment of a crucible from Area C and pictured in Fig. 24 was submitted to ALS USA Inc. in Reno, Nevada, an analytical laboratory specializing in analyses of geologic materials for the mining industry. The sample was crushed and powdered, digested with aqua regia (nitric-hydrochloric acid), and analyzed by inductively coupled plasma atomic emission spectroscopy (ICP-AES). Aqua regia is a partial digestion method designed to remove minerals and elements introduced into a rocky matrix. Elemental values are reported by weight in parts per million (ppm), equivalent to grams per metric ton, and percents (10,000 ppm equals one percent). The results of the analyses are included in Table 1.

### 3.2 Thermoluminescence Dating

A fragment of the same crucible was submitted to the Luminescence Dating Laboratory, Department of Anthropology, at the University of Washington, Seattle, Washington. The laboratory is managed by Professor James Feather. Luminescence dating provides an age estimate for fired ceramic material such as the crucible by determining when it was last exposed to light or heat that was sufficient to reset the preexisting luminescence signal in quartz or feldspar grains. After removal from light or heat, the crystal lattices accumulate defects from ionizing radiation. During analysis, the sample material is again exposed to light or heat and the electrons that were created by ionization and trapped in the lattices are ejected, creating photons of light (luminescence). From this measurement an age can be calculated. To prepare the sample for analysis, the fragment was broken to expose a new surface and drilled at the center with a using a tungsten carbide drill bit. The material then was ground in an agate mortar, treated with HCl, and settled in acetone to separate the 1-8  $\mu\text{m}$  fraction. Analyses were performed on 8 mineral fragments. The sample was measured three ways: thermal luminescence (TL), optical stimulated luminescence (OSL), and infrared stimulated luminescence (IRSL). Dose-rates were based on Guérin et al. (2011). The ages calculated for TL, OSL, and IRSL did not differ at 2-sigma. The results are provided in Table 3 and the full report is available in Appendix I.

### 3.3 Carbon-14 Dating

Three fragments of charcoal collected from the surface at Area C were submitted to Beta Analytic Inc. in Miami, Florida, for C14 dating by accelerator mass spectrometry (AMS). Charcoal fragments were black,

porous, and rock-hard. The laboratory removed carbonates by washing in hot hydrochloric acid (HCl) and organic matter with sodium hydroxide (NaOH). The samples were pulverized to increase surface area. To quote the laboratory procedure:

Sequential injection of Carbon-14, Carbon-13, and Carbon-12 allow for calculation of age both using Carbon-14/Carbon-12 and Carbon-14/Carbon-13 ratios. Simultaneous accumulation of the Carbon-14/Carbon-12, Carbon-14/Carbon-13, and Carbon-13/Carbon-12 ratios ensure ongoing quality control during the detection; the calculation of each provides three different measures to ensure isotope pathway is stable during the analysis. In addition to measuring the Carbon-13/Carbon-12 within the AMS (correction for total fractionation to derive the most accurate conventional radiocarbon age/pMC), the sample's Carbon-13/Carbon-12 ratio is also analyzed in an isotope ratio mass spectrometer. Measurement of the Carbon-13/Carbon-12 ratio allows for correction of the measured Carbon-14 age based on the amount of isotopic fractionation (enrichment or depletion) in the individual sample as compared to the modern standard. If the measurement is not made, one is assumed in the age calculation.

The radiocarbon results were calibrated against tree ring data using the High Probability Density Range (HPD) procedure. The results are provided in Table 2 and the full report is available Appendix II.

### 3.4 Charcoal Species

Two fragments of charcoal from the collection submitted for Carbon-14 dating were examined by archaeobotanist Dr. Caroline Veermerin of the Biax Consult, an archaeological research company in Amsterdam. The samples were broken and examined microscopically. Dr. Veermerin has published on the identification of wood species from the Egyptian ports of Berenike and Myos Hormos, and Roman-age forts in the Eastern Desert of Egypt (Veermerin, 1998; Bouchaud et al., 2018).

### 3.5 Image Processing

The tribal symbols and figures carved into rock surfaces at Jabal Dhaylan were difficult to photograph because of bright sunlight and lack of contrast in the rock surfaces. To improve clarity, all photos of rocks containing petroglyphs were digitally enhanced by adjusting light and contrast, and occasionally rotated to recast the engravings as positives features. For illustrative purposes, each item in the figures was digitally traced in white and the pattern offset to one side. During image processing the texture of some of the images was modified; some made smoother than others, making them appear to be older. Accordingly, the appearance of the symbols in

this report is not a reliable guide to relative age. Copies of the original photos are available on request. Each of the photographs was also examined with DStretch, a private-party image processing utility based on the decorrelation stretch routine that was originally developed for applications in geology. No additional details were uncovered.

## 4. RESULTS AND DISCUSSION

### 4.1 Area A. Stone quarry and tribal symbols

Area A consists of a broad expanse of sand containing few exposures of bedrock. Much of the area is underlain by anhydrite of the Magna Formation, which is mostly exposed where it abuts granitic rocks on the north and south. In the center of the area, at petroglyph site P1, is a narrow, east-west trending exposure of anhydrite surrounded in all directions by sand. 1500 meters to the south is a ridge of Ghawwas formation that has been dissected into an east-trending line of low hills by crosscutting faults. A lithic site is present at a small stone quarry at this location.

#### 4.1.1 Lithic Site

The lithic site (L in Fig. 2) is located on the east flank of the middle of three east-west trending hills composed of Ghawwas formation sandstone and siltstone, each about 10 m high. The two westerly hills were drilled from a distance to test for mineralization at depth. The more westerly hill is flooded with calcite veins, evidence of a high temperature hydrothermal activity that took place early in the opening of the Red Sea (calcite exhibits retrograde solubility and precipitates from solution at high temperature). The hill immediately to the east is locally silicified on its east flank. Here, the rock has been transformed into a rock termed jasperoid, also a product of high temperature hydrothermal activity. The temperature of jasperoid formation is difficult to determine because of the lack of primary fluid inclusions but is assumed to take place at temperatures exceeding 200°C based on the stability of quartz (Lovering, 1972). Jasperoids are typically hard, very fine grained or cryptocrystalline, and produce a sharp edge when chipped. Similar to obsidian, jasperoid is structurally isotropic and can be chipped in any direction.

The silicified area measures about 50 square meters and is littered with thousands of flakes struck from jasperoid cores and exposures of the silicified basement rock. The flakes are remarkably consistent in size. Only a few appeared to be retouched. A single chip was found on the edge of one flake and micro chips were observed on several others. Although mostly unimproved, many of the flakes would function as serviceable blades, scrapers, and awls. Older

tools, such as Acheulean hand axes were not seen, although several round hand-size cutting stones were observed half buried in the sand (which may have been discoid cores). The edges of the flakes are duller than would be expected if chipped from the cores and bedrock exposures (an observation also made by Lloyd Weeks based on the photo in Fig. 3). This is attributed to erosion by windblown sand.



Figure 3. Lithic site, L in Fig. 2. Jasperoid flakes, some with minute secondary chips on edges

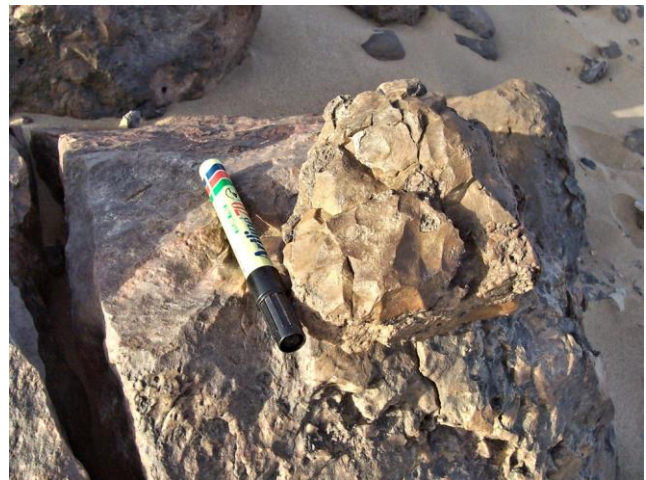


Figure 4. Rounded, flaked silicified core attached to silicified bedrock. Marker is 13cm long.

The predetermined sizes of flakes and inward radial (centripetal) flaking on the core in Fig. 4 is consistent with Levallois tool technology (Crassard and Petraglia, 2014). Levallois tools have been documented in the Arabian peninsula as early as 211,000 years ago and as late as 75,000 years ago (Hilbert et al., 2017, Crassard and Hilbert, 2013). Jasperoids are associated with high temperature, low pressure (epithermal) events that typically codeposit abundant trace elements along with silica, particularly arsenic, antimony, mercury, and thallium. The geochemical signature of the stone may be sufficiently diagnostic to establish provenance.



*Figure 5. Lithic site. Remnants of semicircular structure at center, open to the southeast. View to north. Hammer for scale.*

At the center of the site is the remains of a semicircle of partially buried stones that formed the base of a primitive hut (Fig. 5). Presumably, the hut provided shelter for tool makers. The hut was open towards the southeast, opposite the direction of the prevailing winds. The abundance of flakes and cores suggest that the site was more than a source of tools for local tribesmen but also served as a source of stone for trade goods. Although the site may have been used intermittently for thousands of years, it would be interesting to obtain a date on the structure by applying thermoluminescence dating to the buried sections of the stones. If they date from Levallois time (Middle Paleolithic), the circular structure could be one of the oldest buildings in the archaeological record.

Stone that can be shaped to produce hard, sharp cutting edges is uncommon in most of Saudi Arabia and this isolated site may have been important to early modern humans (EMH) who migrated out of Africa over a million years ago (Bailey, 2009). The crossing at Bab al Mandab between present day Djibouti and Yemen is known to have been an important route out of northeast Africa. Upon reaching the Arabian Peninsula, early man would have headed north into central Asia and east to India, or northwest through the center of Saudi Arabia on the way to the Lavant. A route along the Red Sea coast is also probable, based on the location of some EMH sites and periods of aridity that dried up the lakes along the interior route (Groucutt and Petraglia, 2012).

#### **4.1.2 Cupules and Tribal Symbols**

The location marked P1 in Fig. 2 is an exposure of anhydrite that forms a south-facing ledge about 1 m high. The ledge is discontinuous but trends east-west for about 300 m. The base of the ledge is sheltered from the wind and contains broken slabs of anhydrite that lay flat in the sand. Anhydrite and gypsum are chemical (vs. detrital) sedimentary rocks with the same composition (CaSO<sub>4</sub>). Anhydrite is slightly harder and can be distinguished in the field by conchoidal fracture. During geologic mapping it was discovered that some of the slabs contained engravings (petroglyphs). The symbols were faint and virtually invisible in the dazzling sun (indeed, Sheikh al Jehani admitted to being aware of the slabs for decades but had never noticed the engravings). The location was visited twice, three days apart. Several of the engraved slabs exposed on the first day could not be found on the second day because of drifting sand. This suggests that there are more to be found in the area. Despite many square meters of suitable stone, most symbols were restricted to a few small slabs, and several of the engraved slabs were located hundreds of meters apart. Some symbols displayed ragged, chipped edges, while others were completely smooth and were obviously much older. To record the symbols, photos were taken in the late afternoon to pick up shadow. For the purposes of this report, each photo was computer enhanced and several photos

were also rotated to display the engravings as positive features. A number of symbols were so deeply eroded that they could not be identified. All engravings were digitally traced in white and the outline offset for clarity.

Because the symbols display different degrees of erosion, it is potentially possible to determine their relative ages, the oldest engravings being shallower, more rounded and possessing fewer sharp chip marks. However, the degree of rounding is dependent on how the stone was exposed to the wind, and some of the slabs were more exposed than others. Only for symbols engraved on the same small slab, or on a neighboring slab, can differential erosion be used to establish relative age. The amount of erosion by wind-born (suspended) sand is height dependent, with the greatest amount of erosion a few centimeters above the ground. The anhydrite exposed at the top of the ledge, fully exposed to blowing sand, is devoid of engravings. This also accounts for the erosion seen on the chips at the lithic site, which are fully exposed to the wind. Flat-lying rocks are far less susceptible to wind erosion. Sand grains propelled over the surface by the wind in a hopping motion is termed saltation. Sand that is pushed bodily over the surface is termed creep. No erosion of the surface takes place during creep. Because the anhydrite slabs are flat-lying, located in a recessed area, and are usually partially covered by sand, saltation is the only process that would cause erosion. On low angle surfaces approaching horizontal, the angle of impact of hopping grains is 2-10 degrees to the surface (Bisal and Nielsen, 1961), imparting negligible energy. At wind speeds of less than 11 meters per second (24.6 mph), the amount of erosion on a horizontal surface approaches zero at all impact angles (Bridges et al., 2005). Being protected from the wind except for the minor affects of saltation, the engravings are potentially very old, perhaps thousands of years, despite the fact that anhydrite is relatively soft.

The oldest petroglyphs found at this location are the cupules shown in Figs 6 and 7. Cupules are small cup-shaped indentations pecked or ground into the surface of a stone. Cupules are found in many countries and are considered the oldest type of common rock carving (Bednarik, 2008). Bednarik and Khan (2015) estimate that the cupules that occur in Saudi Arabia date from 9,000-5,000 BP, although cupules have been found that are more recent in age. The cupules at Area A were pecked out with a sharp stone or metal tool, not pounded and ground out with a rounded stone, which is more typical. Peck marks and broken edges are still prominent, which indicate they may post-date some of the symbols on the other stones. The slab at the top of Fig. 7 contains two symbols, a left (handed)-Hook and an open-C. Next to the

left-Hook is what may have been part of a right-Hook that has been intentionally obliterated. The lower slab in Fig. 7 contains a right-Hook and a symbol that has been cut off by the cupule. The identity of this symbol is unknown.



Figure 6. Petroglyph location P1 (Figures 6-12). Cupules in banded anhydrite.

The faint symbols above the cupule in the slab at left could not be identified. Marker is 13 cm long.



Figure 7. Cupules and tribal symbols (wusum) in flat lying slabs of anhydrite.

The right-Hook and open-C are typical of tribal symbols, termed wasm. Wusum (plural) are found everywhere in the Middle East and are often used as brands on camels to denote ownership. They are also used to signify ownership of land by engraving them on rock surfaces. Wusum have been used in Saudi Arabia for 5500 years (Khan, 2000, p.105). Some of the

wasm symbols have their origins in common objects such as a comb (E), a shepherd's staff (Hook), a basket or rope (Key-shape), a horse shoe (Open-C), and roots of a tree (a Cross or Plus sign). Individual symbols are rarely unique to a tribe or clan. A combination of symbols, each specific to a family that is part of a group that stays together, a clan, will not be duplicated elsewhere. Most of the symbols found in the rocks at P1, including those in Fig. 7, can be found in Khan's (2000) compilation of 3,945 wusum found on rock surfaces at 1200 sites in Saudi Arabia. Several of the symbols found at Jabal Dhaylan are also found at nearby towns, all of which are in the domain of the Juhayna tribe. Enhanced images of the major symbols found at P1 were shown to Sheikh al Jehani who, remarkably, identified some of them as belonging to al Jehani families at Jabal Dhaylan. The great age of the tribal symbols at P1, as reflected in their degree of weathering, indicates that the al Jehani clan have been at this location a very long time. The discussion below will show that they have been there since the time of Islam, if not well before

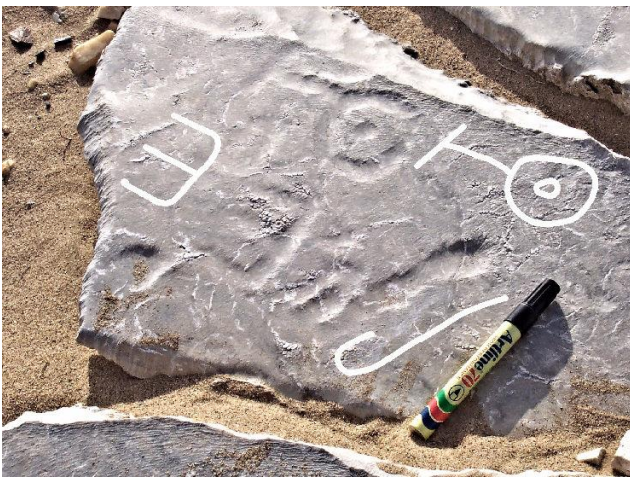


Figure 8. E, Key and right-Hook wasm symbols of the local Bedouin clan. The marker is 13 cm long.

#### 4.1.2.1 Three Families

The symbols on the slab in Fig. 8 are among the oldest in the area based on their degree of erosion. Most chip marks have been eroded smooth and the symbols are shallow in the rock surface. They include three of four recurring symbols that are here interpreted to belong to the patriarchs of the Bedouin families that first settled in Jabal Dhaylan. These include the right-Hook, an E symbol, and a Key symbol. Because the stones are flat-lying, the 'up' position for these symbols is unknown. The Sheikh stated the correct orientation for the right-Hook is with the Hook at the top of the staff. This indicates the orientation of the E symbol in Fig. 8 is open-right. However, the Sheikh disputed this, stating the correct orientation is open-left. As far as the Key symbol was concerned, he

had not seen it before and assumed it was a family that had moved away long ago. This was a prescient observation that will become important later in this report. The E symbol belongs to the family of Hamad Fiede al Jehani, who applies the brand to the left thigh of their camels. The right-Hook symbol is the wasm of the family of his uncle Salman, which means it is also the wasm of the family of the Sheikh, although he did not volunteer this information. Where Salman branded his camels was not investigated.

#### 4.1.2.2 A Fourth Family

Next to the slab in Fig. 8, on a broken piece of the same stone, was found another copy of the right-Hook and a set of inverted-U symbols (Fig. 9). These symbols are substantially less eroded than those in Fig. 8, so they are assumed to have been engraved at a later date. They are interpreted to belong to the fourth family that originally settled at Jabal Dhaylan. The fact that the symbols are accompanied by the right-Hook suggests that the families may have entered the area through marriage. Fig. 9 includes an inverted-U, an inverted-U with sidebar at right, an inverted-V, and 3 small circles. Today, the inverted-U with sidebar is the wasm of the family of Masaid Awada al Jehani, but is shared with his cousin, Hamad. The symbol is applied to the left cheek of their camels. Interestingly, Khan (2000, p. 86) observed that the same symbol is applied to the left cheek of camels by the Juhanina (Juhayna) tribe living at Umlujh (Umm Lajj). Only the inverted-U with sidebar is used as a brand at Jabal Dhaylan today.



Figure 9. Group of inverted-U symbols. Three circular symbols with positive centers preserved at right. Inverted-V symbol at top left. Right-Hook symbol at center left also appears in Figures 7 and 8. The engraving at the left edge of the stone could not be identified. Image processing has smoothed the edges of the symbols.

The inverted-U symbol is found in many locations in Saudi Arabia. To determine how common the other primary symbols at Jabal Dhaylan are--the E, right-

Hook, and Key--an examination was made of thousands of images of petroglyphs from Saudi Arabia that appear in Google Images and Nayeem (2000), and the combinations of tribal brands that are present in Khan (2000). It was found that while the E symbol is common, is always opens down (a comb); no examples were found where it opens to the left or right. In addition, no examples of the E symbol were found with the Key or Hook symbols. As for the Key symbol, no examples were found with a hole in the center of the eye or a cross-bar on the arm, and all were oriented vertically with the head of the key at the top. The association of these three symbols and how they are oriented appears to be unique to al Jehani clan at Jabal Dhaylan, an observation that will allow the families to be identified as participants in a momentous historical event that will be discussed in the section on Area B.



Figure 10. Image of the solitary E symbol with family compound at left. Marker is 10 cm long.

Some of the anhydrite slabs contain quite specific information. For example, in Fig. 10 the E symbol is found next to what is interpreted as a family compound. In this case, the compound appears to contain five or six rooms. If the walls of this structure were constructed with rock or mud and covered with cloth or sticks is unknown. No remains of old structures were observed in Areas A or B.

#### 4.1.2.3 The Extended Families

The relatives of Bedouin families may share a copy of the family wasm that has been amended in some way. An extra line attached to the wasm is termed a shàhid (Khan, 2000). The amendment can denote a separate tribe, a family within a tribe, or a person within a family of the tribe. At location P1, amendments to the E and inverted-U symbols are recorded on several slabs. Examples of similar amendments to the right-Hook and Key symbols were not found. Amendments to the Key symbol were found in Area

B, however, and these will be discussed in that section.

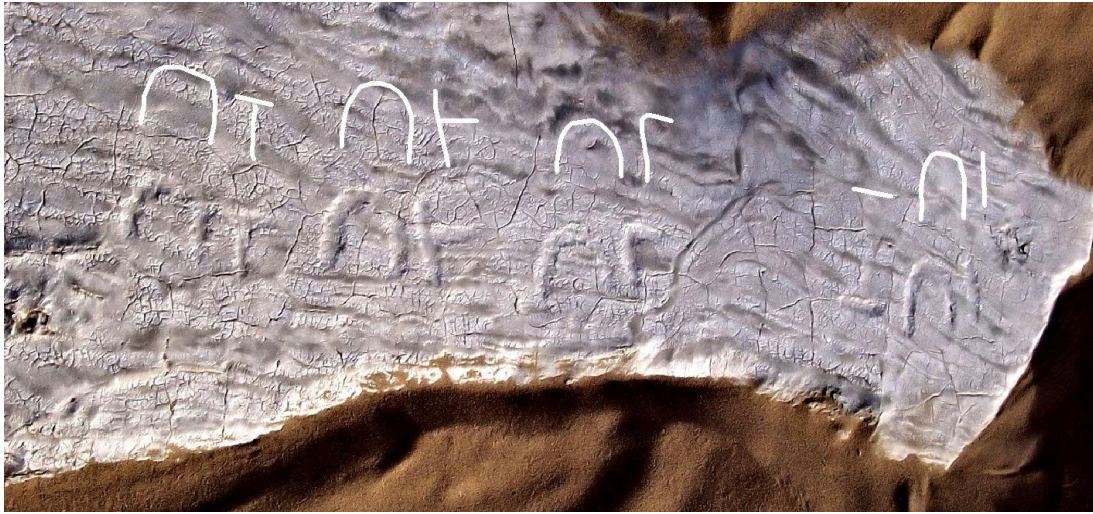


Figure 11. Slab containing three copies of E-hat symbol at left, a different form of E-symbol at bottom right, and a third variant at top center. The open-C symbol is at center. Family compound at right. Hammer head is 17 cm long.

Fig. 11 includes three variations of the E symbol. For simplicity, it will be assumed the E symbols open-right, so the symbols at the bottom of slab are upside down. These include, at the bottom right, an E that contains a line that connects the top arm to the backbone of the symbol. At bottom center, the E symbol contains a small box on the top of the upper arm. This is termed the E-hat symbol. Both symbols are underlined; the one at right with a double line that includes a crossbar. These two E symbols were engraved by scratching with a fine-point tool and minor chipping. The other symbols on the slab appear to have been engraved at a later date and were chipped with a larger tool. The E-hat symbol is duplicated by two larger examples on the left side of the slab. A third variant of the E symbol is present at the top. This symbol contains no additional lines but is associated with a Plus sign. Another symbol is a left-facing open-C at center, similar to the one in Fig. 7. At the right side of the slab is the outline of another family compound. The E symbol at lower right is called 'al Kaffat' and is the wasm of the al Alwazim tribe that lives near Tabuk (Khan, 2000, p. 81). Tabuk is included in the lands inhabited by the Juhayna tribe, so they may be distant cousins to the al Jehani clan. This symbol is also found in the town of Al-'Ula (AlUla), 300 km by land to the northeast. Accompanying this symbol at Al-'Ula are the inverted-U with right sidebar, the downward-facing E, and the vertical Key symbol with no cross bar (Khan, 2000). These shared wusum suggest there is a fundamental connection between Al-'Ula and the al Jehani clan at Jabal Dhaylan. It is noted that the unique Key symbol of the al Jehani (Fig. 8) resembles the giant stone pendant structures located on the basalt-covered plateaus surrounding Al-

'Ula (Kennedy, 2011). The giant wheel-shaped stone structures, also discussed in Kennedy (2011), are represented in a symbol that will be discussed in the section on Area B. The stone tools recovered in archaeological excavations at Al-'Ula are made of basalt and

sandstone (Hausleiter et al., 2021). High quality stone appears to be absent in the area. If high quality 'flint' tools are found, it would be interesting to compare them to the material at the lithic site, L.



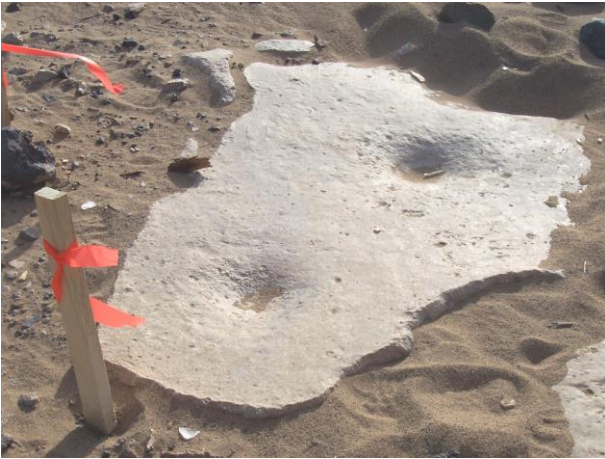
*Figure 12. Rotated image of panel containing four inverted-U wasm symbols, each displaying an additional sign or shàhid that denotes a division within the family. Symbols are the same scale as Figure 9.*

Fig. 12 contains a remarkable set of variations of the inverted-U symbol with right sidebar. These are shown as positive images for clarity. Each sidebar contains a single shàhid. It is tempting to assume that these are the wasm of four sons of the family with the inverted-U with side bar. None of these symbols are used today at Jabal Dhaylan. Because the bedding surfaces in the anhydrite intercept the surface, the symbols are more easily eroded and appear older than they are. The symbol at far right was also found on a small slab on its own.

#### **4.2 Area B. Water**

Area B contains surface exposures of zinc mineralization that were drilled in 2005 and 2006. Several potentially mineable zinc deposits were discovered at depth. With minimal care the archaeological features in the area will not be threatened by mining, if this were to take place in the future. Area B is a rectangular-shaped embayment in the mountain bounded on the east by a wall of granite topped by limestone and claystone and on the north by granite covered with a layer of coral reef debris that slopes down to the south and disappears beneath the sand. The reef material includes bedded limestone sand, several spectacular bioherms, and clastic debris shed from the edge of the coral reef. The assemblage is chaotic and complexly layered, typical of reef slopes. Over time, soft layers have been scoured out by the wind, creating alcoves and overhangs that are sheltered from the prevailing winds that come from the northwest. The northwest-facing side of the mountain immediately north of

Area B is composed of limestone debris that drapes over the granite core. The mineralizing event that produced the zinc deposits blackened the exposures in a manner resembling desert varnish (Hays et al., 2002; Perry and Adams, 1978). Exposed on the desert floor on the west and south sides of Area B is a layer of anhydrite. The layer wraps around the south side of the mountain and is exposed in Area A where it hosts the petroglyphs at location P1. Thickness ranges from less than a meter to over 10 meters based on drilling. Wind-blown sand covers the center of Area B and varies from zero thickness on the west to over four meters deep on the east, based on drilling and dozer cuts. Within the cuts, the sand is crudely layered with thin sections of rocky material shed from the slopes to the east. A cursory inspection found that the rocky layers are devoid of artifacts. The small spring at Area B is the only known source of surface water on the mountain. Except for some wild grass near the spring and a few Acacia trees a few hundred meters south, there is no vegetation. Area B contains a variety of archaeological features but no evidence of ancient structures. No petroglyphs were observed on the blackened limestone exposures facing the northwest.



*Figure 13. Bedrock mortars in anhydrite. Wooden stake is approximately 30 cm long.*

#### 4.2.1 Bedrock Mortars

A small exposure of anhydrite on the south side of Area B contains two bedrock mortars (Fig. 13). They are shallow and bowl-shaped and would have been used for grinding grains, nuts, or dried meat. Alternatively, they may have been used to prepare ochre from red and black zinc gossan exposed a few hundred meters to the north. However, the mortars would have been permanently stained from mineral powder pounded into the surface, and there is no evidence for this. The mortars were exposed by shifting sands; it is likely there are others present, as well

as the stone pestles that were used to pulverize the food items.

#### 4.2.2 Pottery

Fragments of red terracotta pottery were found on the north side of Area B in an alcove sheltered from the wind (Fig. 14). Similar fragments were found on top of a prominent hill on the southwest corner of Area B, and at one of the ancient structures discussed in Area C. The pottery is thick-walled, spun, unglazed and undecorated except for a whitish slip. Gilmore et al. (1985) in Power (2012, p.120) associates this type of ceramic with Umayyad caliphate, 661-750 AD.



*Figure 14. Terracotta pottery shards near spring. Similar fragments were found at one of the shelters in Area C (Figure 26). Hammer is 33 cm long.*



*Figure 15a. Burial cairn, solid white circles in Figure 2. These types of cairns were found on promontories and ridges with expansive views. They are constructed from heavy claystone and appear to be younger than the cairns on the flats (Figure 15b). Hammer for scale.*

### 4.2.3 Burial Cairns

Three piles of dense, dark brown Magna group claystone arranged in circular mounds were found at the top of the ridges above Area B (Fig. 15a, solid circles in Fig. 2). Each location commands an expansive view to the north and west as well as to the flats immediately below. Each mound contains a cone-shaped recess in the top. Similar piles of stone were found on the flats to the northeast but were in poor condition and appeared to be older (Fig. 15b, solid triangles in Fig. 2). These were constructed from boulders of porous coralline limestone that had been carried a few tens of meters from outcrops. At first, the cairns at the high locations were interpreted to be shelters or pits for signal fires. However, Akkermans and Bruning (2017) demonstrated that similar mounds in Jordan are burial cairns. Mustafa and Tayeh (2014) discuss burial cairns in Syria, Jordan, and Arabia, referencing observations of travelers in the 19th and 20th centuries, including T. E. Lawrence (Lawrence of Arabia). Prior to the Bedouins becoming sedentary in the 1960's, nomadic tribes would often carry their dead to high locations located hours or days away so the deceased could look down on the tribe when they camped below. Cairns on the flats were located close to where a person died. Mustafa and Tayeh (2014) report that most cairns include a headstone or flat rock with the wasm of the family. Unfortunately, this was not known at the time. It would be interesting to know if these cairns were marked with the wasm of a local Bedouin family. The age of the cairns is not known. Since becoming sedentary, the Bedouin bury their dead near their camp within a few days of passing, often in unmarked graves. This is the current practice of the al Jehani families at Jabal Dhaylan.

Several burial cairns similar to the one in Fig. 15a are located on a ridge southeast of Area A (Fig. 2). These are constructed from the same dark claystone and contain the same cone-shaped recess at the top. The location commands views in all directions, including the desert floor on the north side.



*Figure 15b. Burial cairn, solid white triangles in Figure 2. These cairns were found on the flats, are poorly preserved, and appeared to be older than the cairns on the ridges (Figure 15a).*

### 4.2.4 Tribal Symbols

On the north side of Area B, approximately one hundred meters up the slope in a sheltered alcove, a group of petroglyphs are carved into a wall of soft limestone sand (Fig. 16). The symbols include a male figure, an Arabic symbol for the letter B, a set of Key-shaped symbols resembling the one in Area A (Fig. 8), a staff-shaped symbol, and a palm tree. Except for the male figure and the staff, which were incised into the rock with an edge of a blade, all of the symbols appear to have been carved with a similar tool, a blade with a flat bottom, square corners, and straight sides. It is assumed that the tool(s) was made of metal and was dragged across the soft surface to make the incisions.

Below the male figure at top left is a single letter of Arabic script (Fig. 16). The style is early Mashq, which is characterized by the elongated horizontal bars at the base of the letters. The script was developed by early Muslims for the exclusive purpose of writing and copying the Quran (Abulhab, 2017) and so dates this inscription as no older than the mid-7th century. Because the letters lack diacritical marks and dots, it was probably carved before the 14th century when Arabic letters were modified to include vowel sounds.



Figure 16. Petroglyphs at location P2 near the spring (Figures 17-19). The panel is sheltered by overhanging rock and faces easterly away from the prevailing winds. Marker is 13 cm long.



Figure 17. Male figure with headdress. White highlights from image processing.

The male figure (Fig. 17) has an elaborate head-dress, drooping arms, and a prominent phallus, the latter which is rare in Arabian rock art and throughout the Middle East. Akkerman communicated personally that of the 5,000 or more rock art figures depicting humans he has recorded in Jordan, only 5 or 6 are embellished with male genitalia. In other parts of

Saudi Arabia, stick figures pecked into stone blackened with desert varnish often include phalluses. The figures are crude and are more accurately described as anthropomorphs. The images are frog-like, with arms and legs projecting at right angles from the side of the body and bent vertically up or down. Examples are found in Nayeem (2000, pgs. 165, 173, 185, 192,

and 295). The figure in Fig. 17 is particularly well rendered and is superior to almost all examples of human figures in Middle Eastern rock art. The head-dress suggests that the figure may represent a shaman. Depictions of humans in sculpture violates the edicts of the Quran which, while not prohibiting the depiction of human figures, it is clear about the portraying objects of idolatry. This is particularly emphasized in the hadiths. If it is assumed the Mashq script was placed after the male figure, the question arises why wasn't the figure defaced. The Guhayna (Juhayna) were one of the first of the Bedouin tribes to abandon polytheism and adopt Islam (MacMichael, 1922), which strongly suggests that the shaman figure predates the beginning of Islam in the 7th century.

The wusum in Fig. 18 are assumed to be the symbols that represent the descendants of the Key family. The Key symbols in Fig. 18 are all rotated from vertical and contain one or more shàhid. The symbol resembling a staff with a curved head is assumed to be the wasm of a family member. It is fortunate that these symbols were found on a vertical surface because knowing the correct orientation of will play an important role later in this report. As mentioned previously, Sheikh al Jehani had not seen the Key symbol

before, which means that these engravings were also unknown to him. The proximity of the Key symbols to the spring suggests this family owned the rights to the spring in the past. Today the spring is owned by the family of Sheikh al Jehani. When the Key family left the clan, ownership may have passed to the right-Hook family, the probable ancestors of the Sheikh.

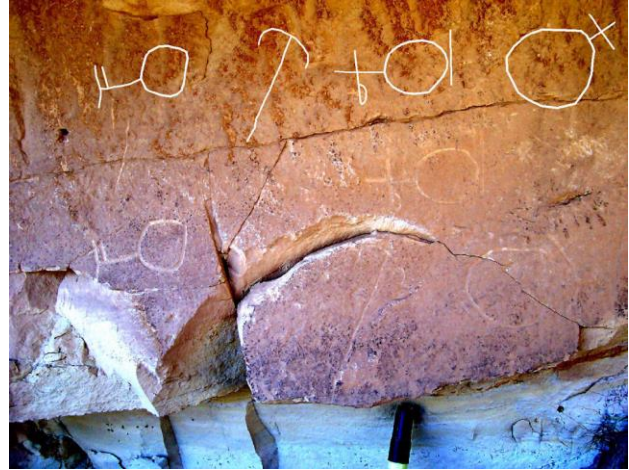


*Figure 18. Wasm symbols. The symbols have been traced in white and offset for clarity. Marker at bottom for scale. The black marks at center right is manganese issuing from the crack in the sandstone.*



*Figure 19. Symbol of a palm tree, lower portion broken away. Top of marker at bottom.*

The other symbol on the panel (Fig 19) is interpreted to be a palm tree, based on similar images in Nayeem (2000, Fig. 235). The lower half is broken

away, but what remains contains no evidence of human appendages such as upraised arms. If such were present, the image might be interpreted as an example of a 'long-haired female', the goddess Queen Alia,

described in Nayeem (2000, p. 333), Bednarik and Khan (2005, Fig. 42), and Kahn (2013, Fig. 15). The presence of the palm symbol suggests that palm trees grew in Area B when the spring flowed more abundantly. This would have made the spring at Jabal Dhaylan particularly important to travelers and nomadic people who could count on abundant water and perhaps a source of dates and grass for livestock. Although it is unknown when the palm symbol was inscribed, date palms were not introduced into Arabia until c 3000 years BC (Tengberg, 2012). A decrease in average yearly temperatures of 2-3°C in the 7th and 8th centuries in the Middle East may have coincided with slightly wetter conditions (Luening et al., 2017, Fig. 2). Earlier periods of wetter conditions in the Middle East are discussed by Rosenberg et al. (2011, Fig. 3). The latest wet phase began 3600 years ago, with desertification beginning 2500 to 1500 years ago.

#### 4.2.5 Connections: The Journey to al Andalus

In this section it will be shown that family members that were once part of the al Jehani clan at Jabal Dhaylan joined an army of Juhayna tribesmen that entered Egypt in the 7th century, and who's descendants were part of the army that invaded Spain in 711-712.

Shortly after the death of the Prophet in 632 the capitol of Islam was moved from Medina to Damascus. Arab expansion began soon thereafter with an expedition south to Egypt in 640 composed of Arab tribesmen, mostly from Syria. Alexandria fell in 642. To follow began the Arab march across North Africa that 70 years later would culminate in the conquest of Spain (al Andalus). In 645 large numbers of tribesmen were brought in from the area of Medina and neighboring Hijaz to secure the lands of Egypt. These included members of the Juhayna tribe (Tāha, 1989, p. 56) and very likely members of the al Jehani clan from Jabal Dhaylan. The new arrivals were not allowed to take up land but were assigned as guards and soldiers at the new Islamic capital at Fustat (in present-day Cairo). However, there is evidence that many members of the Juhayna settled in Upper Egypt following an expedition in 647 (Ahmed-Khalid-Abdallah, 2010), and perhaps sooner by way of the Red Sea (Hassan, 1967, Chapter 5). By 661, tens of thousands of Arabs had migrated into Egypt (Hassan, 1967, p. 33). In 669, a large army was assembled to begin the conquest of North Africa. Most of the soldiers in the army were Arabs that had already settled in Egypt and other parts of North Africa. The army reached Tunisia in 670 and began the construction of the town of al-Qayrawān. Arab tribesmen from different clans selected lots around the central mosque to build their homes. These included soldiers who originally came from Medina, the Juhayna (Tāha, 1989, p. 62). The new city

was reinforced in 679 with 5,000 additional Arab tribesmen from Egypt. In 701, Carthage, 150 km to the north of al-Qayrawān, was captured and the town of Tunis was founded to become the base for the Arab fleet. In 711, Tariq invaded southern Spain by crossing the Strait of Gibraltar from Tangiers in Morocco. Tariq's army consisted of 12,000 men, mostly Berbers from North Africa. The next year, Musa sailed (from Tunis?) with 18,000 thousand men, many of whom came from al-Qayrawān, but also from men from Yaman (Yemen) and other tribes that were already in North Africa (Tāha, 1989, p. 94). This is almost certainly how members of the al Jehani clan entered Spain, as few Arabs were part of Tariq's army that crossed the year before.

Many of the Berbers and Arabs who conquered al-Andalus settled in the new lands. Where they settled and to which tribe or clan they belonged is well documented in ancient Arab texts (Tāha, 1989, Chapter 4). They are referred to as the early settlers (al-baladiyyūn). Relative to the other Arab tribes who first entered Spain, only a small number were from the Juhayna tribe. It is known that they settled in Cordoba (Tāha, 1989, p. 127) and it is here where we find evidence of the al Jehani clan. That the Juhayna were a minor part of the army that invaded Spain suggests that the bulk of the Juhayna stayed in Egypt and the Sudan. By 1400 the Guhayna (Juhayna) were the largest tribe in Upper Egypt (MacMichael, 1922, p.138).

In 2004, a stone monument approximately a 1.5 meters tall and covered with symbols was discovered in a pile of loose stones that had been removed from a farmer's field two years before (Fig. 20). The location was near Montoro, 35 km northeast of Cordoba, and the monument was duly named the stela of Montoro (Sanjuan et al., 2017). The stela contains 31 symbols that are separable into five groups based on how they were engraved (pecking, abrading, or incision) and the order in which they were engraved on the stone. Most of the symbols are assumed to be graphemes (symbols that represent a sound in a language). The symbols in the first four sets, the earliest, resemble those that appear on other stela in the Iberian peninsula and can trace their origins to Phoenician, Graeco-Iberian, and Palaeohispanic scripts. Part of the last set to be inscribed, highlighted in white in Fig 20, had not been seen in Spain before. To the authors, several symbols appeared to be vaguely oriental and proposed they had their origins in first millennium BC Proto-Canaanite, Proto-Sinaitic and South Arabian scripts. These symbols most closely match the northern variant of the South Arabian scripts, the Thamudic languages (Khan, 1991; Nayeem, 2000, Chap. XVII). The Thamudic languages have their origin in the Bedouin wasm symbols and Thamudic B, in particular, resembles the symbols on the stela.

The authors assumed all the symbols dated from the third to first millennium BC, with the majority from the Iron Age (800 to 600 BC) based on other occurrences in Iberia.

The symbols highlighted in white in Fig. 20, except those indicated by an arrow, resemble many of those found at Jabal Dhaylan. These are compiled in Fig. 21. The orientation of the highlighted symbols is assumed to be upside down based on the staff symbol, which in Fig. 18 is orientated with the cross bar at the top. Rotating the stela top to bottom results in the orientation of the symbols reproduced in the bottom row of Fig. 21. If the wasm-type symbols on the stela were added last, as concluded by Sanjuan et al. (2017), their location at the top of the stone is inconsistent with most forms of writing, which start at the top of the medium and work down, with unused space left at the bottom. While some of the symbols on the stela are poorly defined, they are carefully reproduced in Sanjuan et al. (2017). Each of the highlighted symbols have an exact or close match in the al Jehani family tribal symbols, as shown in Fig. 21. If only one or two symbols on the stela matched those from Jabal Dhaylan, one could argue it was a coincidence. To find representative symbols from all four families is indisputable evidence that the stela was engraved by members of the al Jehani clan from Jabal Dhaylan, most probably in the year 712 or shortly thereafter.



Figure 20. The stela of Montoro, Spain. Symbols assumed to be the same age are highlighted, but also include the large Key-type symbol at center and several of the straight lines. Except for the two symbols indicated by the arrows, all of the highlighted symbols are found at Jabal Dhaylan.

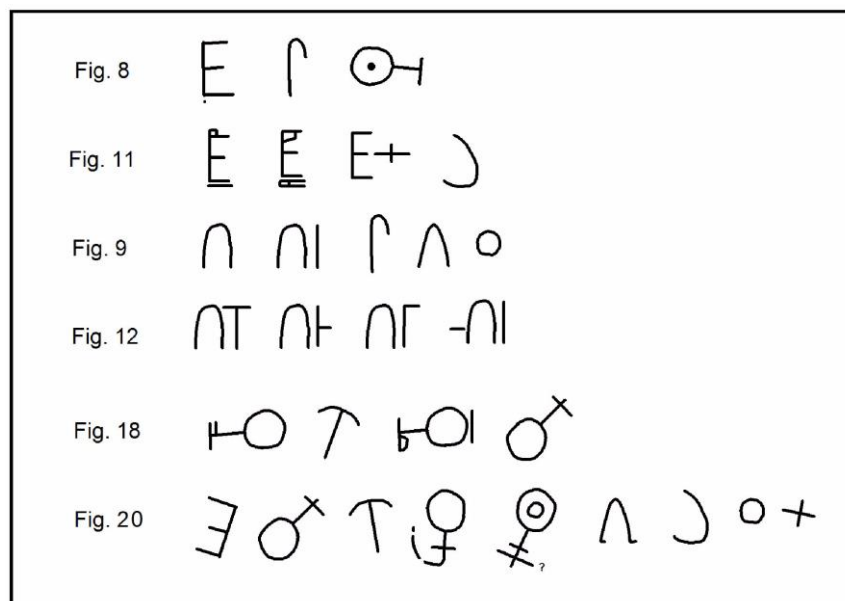


Figure 21. Compilation of tribal symbols from petroglyphs in Area A and B at Jabal Dhaylan (Figures 8, 9, 11, 12, and 18). Selected tribal symbols from the stela of Montoro in Figure 20 are exact or close matches.

Of the four families represented in the petroglyphs at Jabal Dhaylan, the largest number of symbols on the stela belong to the Key family, the very family Sheikh al Jehani proposed had left Jabal Dhaylan sometime in the distant past. The fact that all the families from Jabal Dhaylan are represented on the stela of Montoro indicates that those who left Jabal Dhaylan included members from each family, not just the Key family. The symbols include the E symbol, which in this case opens left, the correct orientation according to the Sheikh. This family is also represented on the stela by the open-C and Plus sign. The inverted-U family is represented by two symbols, the inverted-V and a small circle. The right-Hook family is probably part of the inverted-U family, as is suggested in Fig. 9. Two symbols are indicated by arrows. The one at left resembles the Wheel, which is one of the types of monolithic stone patterns found on the basalt plateaus surrounding Al-'Ula (Kennedy, 2011; Thomas et al., 2021). The symbol on the right is a letter from the Dadanitic alphabet, the script that was used at the oasis of Dadan, today's Al-'Ula. It should be noted that the right-Hook symbol is also a letter in the Dadanitic alphabet (Macdonald et al., 2017, p. XIV). The vertical dumbbell-shaped symbol on the right side of the stone dates from the Dadan period as well. If members of the al Jehani families originated in Al-'Ula, migrated to Jabal Dhaylan, and later travelled to Islamic Spain, it would not be surprising if they retained symbols from their homeland. What is remarkable is that the people who settled in Spain were not the ones who left Jabal Dhaylan. Rather, it was their grandchildren or great grandchildren. The successive generations retained their family tribal symbols, probably by keeping camels in Egypt. The presence of the ancestors of the al Jehani clan from Jabal Dhaylan in al Andalus may be the only known example of a direct connection between a living Arab Bedouin clan and ancestors that settled in Spain in the early years of the conquest. Today, approximately 8% of the DNA of Central and Southern Spaniards is identified as Red Sea Bedouin origin, including Yemenite. Of this, 6% is attributed to admixture during the Arab conquest and 2% from the Phoenicians, who were part Bedouin (Hay, 2017).

#### 4.3 Area C. Ancient Mining

This location (Fig. 2) contains substantial zinc deposits that were first explored by the French in 1968-1972 and later by the United States Geological Survey in 1996-2000 (Hayes et al., 2001, 2002). The area was drilled by Petro-Hunt Middleeast Co. in 2005-2006, and although the deposits were expanded in size, they remained uneconomic at current metal prices. The deposits consist of the zinc sulfide, sphalerite (ZnS), that was codeposited with black cryptomelane,

a complex zinc-bearing potassium-manganese oxide. The zinc deposits are thoroughly oxidized and only secondary zinc minerals are found at the surface. These include hemimorphite, a zinc silicate, and the zinc carbonates hydrozincite and smithsonite. The latter two minerals were historically termed calomine and occur as veins and irregular masses on Calomine Hill. Primary mineralization also includes lead in the form of the lead sulfide, galena (PbS), which is present as narrow, 2-3 cm veinlets in the limestone. Most galena exposed at the surface is oxidized to cerussite, a lead carbonate. The deposits are hosted by reef limestone of the Magna group and are located on Calamine and Cryptomelane Hill and exposures on the west side of the mountain. Today we know that depending on how galena is deposited (the type of mineral deposit), it may contain thousands of grams of silver per ton or almost none at all. At Jabal Dhaylan the lead and zinc is associated with what is termed a salt-related, carbonate-hosted Zn-Pb deposit, formed from metalliferous brines that were generated in the Red Sea during rifting in the Miocene. Lead-zinc deposits formed at rifting centers typically contains less than 20 grams silver per ton of sulphide (Kyle and Price, 1986). Hayes et al. (2002) determined the average lead-zinc ore in Area C contained 5 grams of silver or less. Thin veins of galena in similar age rocks across the Red Sea on the Egyptian coast are also deficient in silver. The deposits of Gebel El Rosas and Umm Gehig contain 16 grams of silver or less per ton of lead sulfide ore (Stos-Gale and Gale, 1981). Pernicka et al. (1998) estimates that in the Early Bronze Age of the Aegean (3000-1200 BC) at least 500 grams of silver per ton was required make it feasible to extract silver from lead-silver ore. This is far more than is present in the lead-silver ore in Area C. Petro-Hunt did not include silver in their analyzes of lead and zinc, knowing a priori that the amounts would be insignificant based on the geologic environment. The type of zinc deposits at Areas B and C are the same, but differ from the jasperoid occurrence at Area A by being associated with low temperature brines that traveled far from the centers of rifting in the Red Sea.

#### 4.3.1 Silver Mining and Smelting

In ancient times, any occurrence of galena would have been tested for silver. Despite the presence of abundant lead and zinc minerals at the surface at Area C, no mention of ancient mining or smelting had been recorded for the area, including the comprehensive survey of ancient mining sites in the region by Sabir (1991), and the work by the French and American geologists. Hayes et al. (2002), in particular, found it curious that for the many exposures of secondary lead and zinc minerals, and occasional veinlets of ga-

lena, there was no evidence of past mining or the remains of a mining village. The reason is that prior to 2005-2006 all geological work had been performed on the west side of the mountain. In 2005, a road was constructed between Calamine and Cryptomelane

Hills, indicated by the dashed line in Fig. 2. The road exposed the remains of silver smelting on the east of Cryptomelane Hill (Fig. 22), and a few hundred meters further east were the remains of a village (Fig. 25).

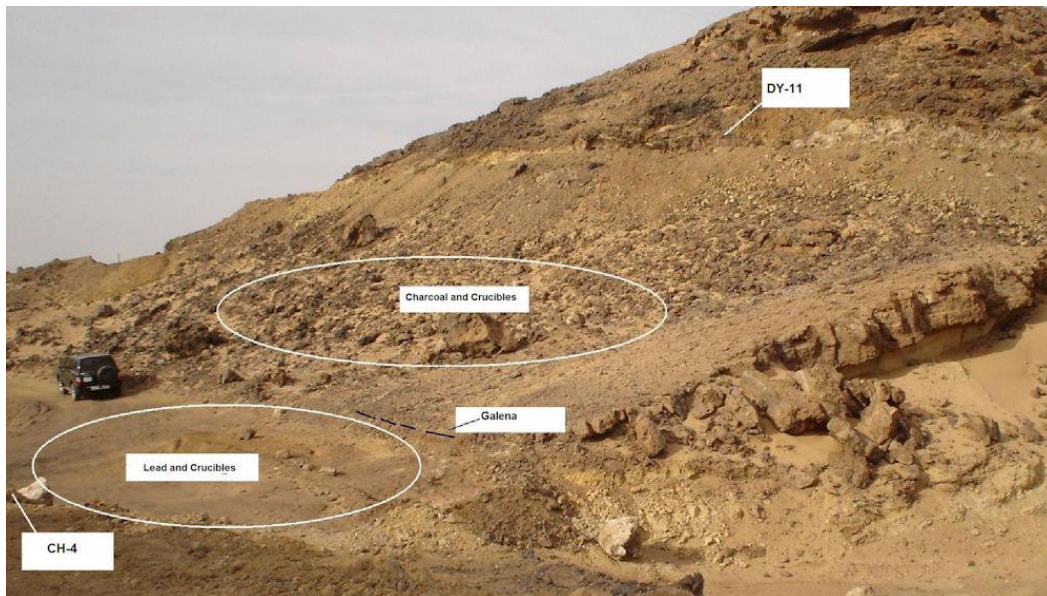


*Figure 22. Site of ancient mining and smelting, view to northwest. Recent roadwork and drilling have exposed the remnants of ancient mining and smelting. Galena (lead sulphide) was extracted from narrow veins above the present roadway and near the location of drill hole DY-11. Minor galena was also found at shallow depth in drill hole CH-4. Cryptomelane Hill on the right.*

Galena invariably contains a certain percentage of silver (argentiferous) and Bedouins or prospectors would have tested any occurrence for its silver content by cupellation, a simple process that utilizes local materials and can be accomplished in a day or two. Cupellation dates from the mid-5th millennium on lead ores in Romania (Hansen et al., 2019), and the mid-4th millennium BC from locations in Turkey, Syria, and Iran. By mid-4th millennium BC silver objects began to appear across the Middle East, which indicates the procedure for winning silver was already known, although the silver may have been obtained from primary silver sulfide minerals such as argentite rather than lead ore (Weeks, 2012). Similarly, silver from 4th millennium BC Predynastic Egypt was determined by Gale and Stos-Gale (1981) to contain gold and thus came from Egyptian gold-silver ores, not veins of galena. Abundant evidence that cupellation took place at Area C is present in broken crucibles (cupules), metallic lead, and partially roasted ore (Fig. 23).

To test the galena for silver, the lead ore would have processed by a procedure described by Anguilano et al. (2010) whereby fragments of galena and/or cerrusite were broken into small pieces, heaped on a bed of wood, and burned in the open air to oxidize the lead sulphide to lead oxide. Galena fully converts to lead oxide at about 900°C and melts, coalescing into

a molten mass in the fire. In the open air, atmospheric oxygen maintains part of the molten lead as an oxide, but carbon monoxide given off by burning charcoal reduces some of it to metallic lead, which flows from the mass in fingers called runnels. Silver would be present in both fractions. When the fire cools, the residuum consists of lead oxide mixed with ash, charcoal, and rocky material, fragments of which are present in Figure 23 (here termed slag). The runnels are placed in small crucibles (cupules) fashioned from local sand and heated to approximately 1000°C with the aid of a blowpipe. The lead melts and is converted back to lead oxide in the presence of oxygen, migrates into the porous walls of the crucible, combines with silica to form a glaze, or is driven off as a gas. Silver, if present, collects as a small bead in the bottom of the crucible. The heat from the blowpipe would be sufficient to melt silicate minerals on the exterior of the crucible, which may turn green from the incorporation of lead. Fig. 24 shows several samples of crucible with external surfaces blackened and turned to glass (vitrified) by the intense heat. These materials were collected from the area marked Lead and Crucibles in Fig. 22. Tools that would have been used for mining, such as iron chisels or picks were not observed in this area, although a search was not made for these types of items.



Figure 23. Fragments of crucibles (red) were used to reduce galena to lead (black) at location indicated in Figure 22 as Lead and Crucibles. Pen is 14 cm long.

Evidence that the galena contained little or no silver includes a lack of large vessels that would have been used to reduce the ore in a controlled atmosphere and fragments of higher quality crucibles made of clay. In addition, the crude, locally made crucibles in Figs 23 and 24 would have been recycled to extract any contained silver. If silver was present, oxygen would have been infused into the molten lead with a blowpipe or by stirring in a closed container. This would have created the lead oxide mineral, litharge, which is red-orange in color. Litharge is not present in Fig. 23. The yellow mineral in the figure is probably the dimorph of litharge, massicot. Massicot is a product of thermal oxidizing of cerrusite at temperatures less than 470° C (Worthing and Sutherland, 1996). The white mineral in the figure is hydrozincite, which is abundant in the area. The discovery of recoverable silver would have led to mining of the veins of galena. There is no evidence of pits or trenches on the west or east side of Cryptomelane Hill. Ancient miners wouldn't have known that the lead ore was deficient in silver, and it is likely that the galena from Cryptomelane Hill was tested numerous times over the ages. That this took place will be demonstrated in the section on Dating below.



Figure 24. Fragments of crucibles (top) fashioned from local sand displaying dark glassy rims produced by intense heating. Below, mass of lead from bed of roadway in Figure 22. The fragment at top left was used for elemental analysis and thermoluminescence dating.

#### 4.3.1.1 Trace Elements

Analytical work was performed on the fragment of crucible shown at the top left in Fig. 24. The fragment was broken normal to the outer surface and one half submitted to ALS Labs in Reno, Nevada, for major and minor elements. The results in Table 1 show the walls of the crucible are impregnated with lead, as would be expected if was used to extract silver from lead oxide. The crucible also contains three percent zinc, consistent with the ore being a lead-zinc mixture, and almost one percent manganese (Mn), which came from cryptomelane. Assuming the lead that mi-

grated into walls of the crucible contained some silver, the analysis should provide an indication of the silver content of the lead ore. The value of 7 ppm silver (Ag) is the same low value obtained on lead-zinc

ore (5 ppm) by Hayes et al. (2002, p.32) and indicates that little or no silver was separated in the cupellation process.

Table 1. Major and Minor Elements in Crucible Fragment

Elements Percent (10,000 ppm)											
Al	Ca	Fe	K	Mg	Mn	Na	Pb	S	Ti	Zn	
1.52	3.29	1.54	0.34	1	0.88	0.59	>20.0	2.27	0.12	3.06	
Elements ppm											
Ag	As	Ba	Be	Bi	Cd	Co	Cr	Cu	Ga	Hg	
7	<10	120	<5	<10	182	7	25	24	<50	<5	
La	Mo	Ni	P	Sb	Sc	Sr	Th	Tl	U	V	W
<50	<5	21	300	<10	5	636	<100	<50	<50	37	<50

### 4.3.2 Dating

The area in Fig. 22 is replete with broken crucibles, partially roasted lead ore, fragments of charcoal, and pieces of galena. The site was obviously visited many times as it only takes a few days to test a sample of galena for silver. When did these activities take place? To answer this question, age dates were obtained on a sample of broken crucible and several pieces of charcoal.

#### 4.3.2.1 Thermoluminescence

The remaining half of the fragment of crucible in Fig. 24 submitted for trace elements was analyzed at the Luminescence Dating Laboratory at the University of Washington in Seattle. Luminescence dating provides an age estimate for fired ceramic material such as the crucible by determining when it was last exposed to light or heat that was sufficient to reset the preexisting luminescence signal in quartz or feldspar grains. The sample was measured three ways: thermal luminescence (TL), optical stimulated luminescence (OSL), and infrared stimulated luminescence (IRSL). The ages calculated for TL, OSL, and IRSL did not differ at 2-sigma. The result for the weighted average date was 5810 years BP +/- 560 years, or 3800 +/- 560 years BC. This extraordinary date coincides with the earliest known dates for extracting silver from lead ore by cupellation in Syria and Anatolia (Craddock, 2014). This date also demonstrates that every rock exposure in Arabia, however remote, had been checked for valuable metals by the 4th millennium BC, if not many centuries earlier.

#### 4.3.2.2 Carbon-14

Small scatters of charcoal and fragments of galena were found on the side of Cryptomelane Hill at the location marked Charcoal and Crucibles in Fig. 22.

Several fragments of charcoal were collected from three locations spaced 4-5 m apart. The fragments of charcoal were black, porous, and rock-hard. Two pieces were examined by Dr. Caroline Veermerin of the Biax Consult and identified as coming from the Leguminosae family, which includes the Acacia, the only tree in the area today except for small clusters of date palms kept by Bedouins and watered from wells. There are no Acacia near the site, the closest being in Area B near the spring. Carbon-14 age dates for the charcoal at each location were determined at Beta Analytic Inc. in Miami, Florida. Analyses were performed by accelerator mass spectrometry and isotope ratio mass spectrometry. Carbon-14 dating determines when a plant died, not when it was burned. In the deserts of Saudi Arabia, wood suitable for fuel is scarce, so it can be assumed the wood did not lay around long before it was collected. Table 3 contains Carbon-14 dates from the three locations. The averages of the 7th century dates for samples Jabal 1, 2, and 3 are 692, 670, and 633 AD, respectively. These dates coincide with the initial expansion of the Arab empire under the Prophet Muhammad. Heck (1999) examined the spread of the Islam empire and concluded it was financed by gold and silver. From the earliest days, every significant occurrence of gold and silver was mined to obtain precious metals. The lead occurrences at Jabal Dhaylan, being only 300 km from Medina by land, and within the lands controlled by the same tribe, the Juhayna, were evaluated early during the rule of the Prophet, based on the Carbon-14 dates. The carbon dates in conjunction with the date for the crucible demonstrate that Area C was visited numerous times over the centuries. Since it is unlikely that knowledge was passed on, each new generation of prospectors tested the lead ore for silver, only to find that none was present.

Table 2. Carbon-14 dates for three charcoal samples

Sample	Total Probability		Calibrated Date AD	Calibrated Date BP		Calibrated Date AD	Calibrated Date BP
Jabal 1	95.4%	64.4%	660 - 730	1290 - 1220	31.0%	736 - 770	1214 - 1180
	68.2%	46.4%	668 - 710	1282 - 1240	21.8%	745 - 764	1204 - 1186
Jabal 2	95.4%	88.5%	636 - 714	1314 - 1236	6.9%	744 - 765	1206 - 1185
	68.2%	68.2%	650 - 680				
Jabal 3	95.4%	95.4%	597 - 670	1353 - 1280			
	68.2%	68.2%	620 - 659	1330 - 1291			



Figure 25. Remains of six stone shelters located 100 m east of location of ancient mining in Figure 22. Arrow shows location and orientation of photo in Figure 26. View to the southeast from top of Cryptomelane Hill.

### 4.3.3 The Village

The remains of a village are located immediately east and below the area shown in Fig. 22. The presence of the village is perplexing, considering that prospectors would have quickly discovered that galena in the area is devoid of silver. What was the purpose of the village if not for mining? The walls of the buildings were constructed with blocks of limestone carried from the hills to the north. Hundreds of stones are present in each building, and at least a thousand stones were carried in to construct the multi-room structure at the lower right in Fig. 25. This structure also contains the remains of an enclosure on its west side, most likely to contain sheep or cattle. These were not temporary shelters built by nomadic people. There is no surface water near the village. Because the location is high on an alluvial fan, well water would be out of reach. The drill holes in Fig. 22 and others penetrated to depths below the elevation of the village and did not encounter water. Today, the nearest water is the wadi 2.5 km to the east, where shallow wells are present at the center of several walled compounds (w in Fig. 2). This is the same distance to the

source of water in Area B. Assuming that each of the six buildings housed a family and each room was occupied, the village could have housed 20 or more people. Alternatively, the village may have been occupied by a few people at any one time: as new families arrived, they built their own shelter, choosing not to occupy an abandoned building or pilfer the stones to build their own. If the buildings date from the time of Islam, either option would have been considered theft of personal property, which carries a heavy penalty in the Quran (5:38). In the foreground of Fig. 26 is the remains of one of the shelters. Fragments of pottery identical to those found in Area B (Fig. 14) were found on the surface at this location. The remains of the multi-room structure are in the background near the vehicle. The dated charcoal came from the area where galena was processed for silver, not the mining village. The age of the village is unknown but the type of pottery suggests sometime during the time of the Umayyad caliphate, as discussed in the section on Area B. The location marked P3 will be discussed below.

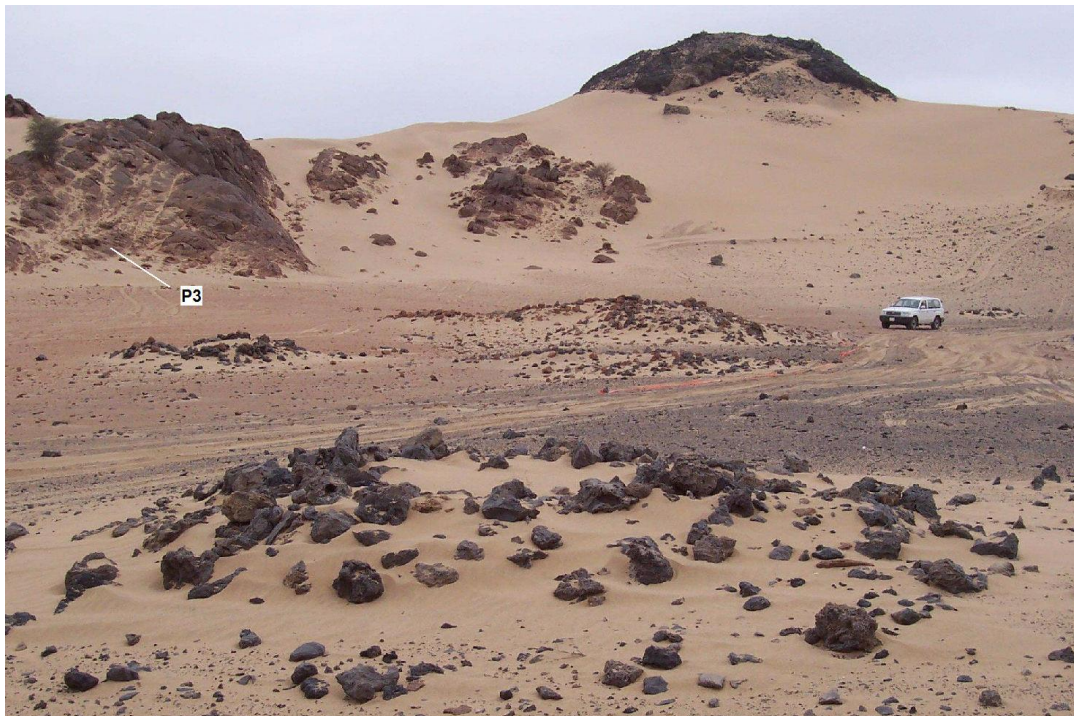


Figure 26. Ground view of shelters, view to west. Location of mining is at top right, off photo. Calamine Hill, top center. Location of petroglyph P3 is indicated.

#### 4.3.4 What was Mined?

Assuming the buildings housed miners, the other potentially valuable commodities at Area C include kohl or metallic lead from galena, manganese oxide (cryptomelane), and secondary zinc minerals.

An important problem in archaeology is identifying the provenance of metals in metal artifacts such as coins, jewelry, and various utensils. This task can be reversed by attempting to locate metal artifacts made from a particular ore, such as lead, silver, copper, or tin. A widely used procedure is to measure the lead isotopes of ore samples and artifacts and search for a match in the isotope ratios. Virtually all rocks and minerals contain traces of lead and the value of the four major isotopes of lead, atomic weights 204, 206, 207, and 208, can be measured with great accuracy by mass spectrometry. The isotopes of lead do not fractionate during mineral processing, including smelting. At any one mining site, the values of the lead isotopes in the ore minerals will vary (Killick et al., 2020), but the limited range of values at many sites is distinctive, and although they may not exactly match the ratios in an artifact, the source of the metal can be established with some confidence. If trace elements are also determined on the ore mineral and artifact, specific trace element ratios in conjunction with isotope ratios can establish the location with certainty (such as the values for cadmium (Cd) and strontium (Sr) in Table 1). Ideally, mining sites should be characterized by five or more lead isotope determinations. These

values will plot on a isotope ratio diagram as a straight line (isochron) and metal originating from the deposit will fall along this line. The zinc deposits at Jabal Dhaylan contain minor amounts of lead as galena or cerrusite, but the lead isotope ratios will be the same (or very similar) in all primary and secondary zinc and lead minerals, as well as manganese where lead is present as an impurity. If an artifact or scrap of metal at another location is found to have the same lead isotope ratios, the metal probably came from Jabal Dhaylan, an exciting discovery that potentially establishes a trade route. However, if metal extracted from ore at Jabal Dhaylan is mixed with metal from another location, the unique isotopic signature is lost and a correlation, with few exceptions, becomes impossible.

At Jabal Dhaylan, lead isotope ratios are available for a single sample of galena (Doe and Rohrbough, 1977, sample Dhaylan, p. 67). The values are listed in Table 3. Trace element data is not available for this sample but the data obtained on the crucible in Table 1 should be representative.

Table 3. Lead isotope ratios for Jabal Dhaylan galena. Values for Pb 207/206 and Pb 208/206 were calculated from the other ratios

Pb <sup>206</sup> /204	Pb <sup>207</sup> /206	Pb <sup>208</sup> /206	Pb <sup>207</sup> /204	Pb <sup>208</sup> /204
19.376	0.806	1.996	15.626	38.681

Minerals that may have been processed at Area C include galena, which in finely powdered form was

used as a treatment for eye infections (surma). Lead sulfide is toxic to bacteria and its use as a medication for eye infections dates from the Bronze Age in Egypt (Catherine, 2005). Arab Bedouins applied powdered galena around their eyes to lessen the glare of sunlight, and directly to the eyeball to treat eye infections (Mahmood et al., 2009). Another use of powdered galena was as an eye shadow (kohl), the earliest examples of which are found in wall paintings featuring females with dark eyes from the Early Dynastic Period (3150-2650 BC) in Egypt. The first kohl boxes date from the 3rd millennium BC from Gypt in Upper Egypt (Sahin, 2020). Galena was so prized that it was placed in Egyptian graves as early as 4000 BC (burial galenas). Some Egyptian kohls have been found to contain smithsonite (calamine) and manganese (Riesmeier et al., 2022), which are both abundant in Area C.

Metallic lead, relatively free of impurities, was found at the location marked Lead and Crucibles in Fig. 22. An example is shown in Fig. 24. There are few lead isotope analyses for artifacts or pure metals from Saudi Arabia, so it cannot be determined if metallic lead was purposely extracted from galena and sold or traded elsewhere in the peninsula. However, many isotope determinations are available for lead objects from Egypt. Occurrences of galena in Egypt are rare and most are located on the coast south of Quseer (El Qoseir). The distance by land from these mines to Lower Egypt is the same distance from Jabal Dhaylan, which is by a much easier route. Another route to Egyptian markets was directly across the Red Sea to the port of Quseer and Wadi Hammamat, which leads inland to Upper Egypt and the city of Thebes. Shipborne trade across the Red Sea was well established by this time (Boivin and Fuller, 2009). In Egypt, little metallic lead appears in prehistoric times. Various lead and silver objects and fragments of galena have been recovered from Predynastic (3750-3100 BC, Dee et al., 2013) tombs in the neighborhood of Thebes. In the 12th Dynasty (1938-1756 BC) caravans of Bedouins from the Egyptian Eastern Desert traded galena for goods (Bard and Fattovich, 2015). Lead was used for metallurgical purposes to suppress the melting points in copper-tin alloys (bronze) starting in the Middle Kingdom (2040-1782 BC), and in the 19th Dynasty (ca. 1292-1189 BC) the use of lead became widespread, coincident with the Bronze Age (Odgen, 2000).

Lead isotope values have been obtained on a variety of Egyptian artifacts, glasses, kohls, burial galenas, and lead ores. Most of these results and are presented in Shortland et al. (2006). The isotopic composition of Jabal Dhaylan lead is very similar to Egyptian kohls from the 18th Dynasty (1550-1292 BC) (Shortland, et al., 2006, Fig. 2b), indicating a possible

match. However, the values fall just below the isochron that is associated with the lead ores from Gebel Zeit on the Egyptian coast, which Hays et al. (2002) describe as being of the same age and type as Jabal Dhaylan. The slight difference in the isotope ratios between the two deposits can be attributed to sub-regional variations in the composition of the Arabian Shield rocks that underlie the Red Sea, from which the lead ores inherit their isotopic signature.

Lead was also used extensively in Islamic times as an additive in glazes applied to ceramic vessels. The provenance of lead in Islamic glazes has been studied extensively Mason et al. (1992), who has identified sources all over the Middle East, including Saudi Arabia. However, none of the isotopic values are close to the values at Jabal Dhaylan or the Egyptian lead deposits. Similar results were found for Islamic-age glazes from the Egyptian city of Fustat dating from the 8th through 14th centuries (Wolf et al., 2003). Apparently, lead was readily available from other countries.

Manganese dioxide ( $MnO_2$ ) is a common mineral and is found in numerous geologic environments. Its association with lead and zinc at Jabal Dhaylan is unusual and the three elements together in an ancient product such as a glaze or cosmetic would suggest a connection. Manganese oxide is soft and black. When powdered it would resemble kohl made from galena. However, it does not absorb UV radiation and has no antibacterial properties. Manganese oxide is also an eye irritant, whereas powdered galena is not. The manganese oxide, pyrolusite, is found with lead in cosmetics in the Royal Tombs of Ur in Iran, which date from 3800 BC (Bimson, 1980). The compounds contained only minor amounts of zinc, which is not consistent with the Jabal Dhaylan zinc-manganese ore (Hauptmann et al., 2016). Manganese was used to decolorize glass from the 1st century BC to the 5th century in the Near East (Swann et al., 1989). Bronze Age Egyptian cobalt blue glass with high zinc and manganese have been found at Malkata (Shortland et al., 2006). The manganese is considered to be a colorant and is correlated with zinc, suggesting the colorant was a manganese-zinc mineral. However, zinc is also correlated with nickel and cobalt, which occur together naturally. The source of the cobalt and associated elements has been traced to two sites in Egyptian western desert (Hodgkinson et al., 2020) but the origin of the manganese has not been established. Because the manganese at Jabal Dhaylan is bound with zinc, this cannot be the source.

Despite extraordinarily rich zinc-manganese ore exposed at the surface at Cryptomelane Hill, there is no evidence the ore was mined or processed for zinc. Zinc metal boils at  $913^{\circ}C$  and must be distilled from a gas, a process that may be inhibited in the presence of

manganese. There is no evidence of distillation at the site, such as retorts described by Craddock et al. (1985). Zinc was not known to be a unique metal until the 14th century and manganese was not isolated as a metal until 1774.

Calamine brass is a low-zinc alloy of copper that was popular in ancient times because of its color, which is similar to gold. It was particularly popular with Arab Muslims. Before metallic zinc was readily available hundreds of years after its discovery in the 14th century in India, zinc was added to molten copper to form brass by the cementation process. This process dates from the 3rd millennium BC in the Near East (Thornton and Ehlers, 2003), but became widespread in the 1st century BC (Weeks, 2004). Cementation utilized zinc contained in the natural oxidation products of sphalerite: smithsonite and hemimorphite (calamine). Alternatively, cementation used synthetic zinc oxide, zincite, which was created by roasting sphalerite to form zinc vapor (sublimation) and combining the vapor with oxygen in the presence of extra air to form a powder. Brass made from calamine will contain impurities such as iron and manganese that were included in the zinc ore, whereas brass made from zinc oxide will be free of impurities except for small amounts of lead that typically occurs with zinc. Brass from Europe, made in great quantities by the Romans from calamine mined in Anatolia (northern Turkey), the Italian Alps, and later Spain (Morton, 2019), can be distinguished by anomalous amounts of iron and manganese. Because these sources of calamine were not accessible to the Arabs until the 9th century, brass from the Near East was made from zinc oxide and is free of iron and manganese (Ponting, 1999; Craddock et al., 1998). Brass from the Middle East that dates before the 9th century that contains iron and manganese is assumed to have arrived by trade. In the 9th century, Arab armies captured Anatolia and the composition of Middle East calamine brass began to resemble Roman products that contained minor amounts of iron and manganese.

Prior to the 9th century, it can be assumed that any source of natural calamine in the Near or Middle East would have been exploited, rather than having to have to trade for zinc oxide, which primarily came from Persia. Calamine from Jabal Dhaylan could have easily been transported to markets in Egypt and other Near East countries. Brass made from this material would contain high amounts of manganese and lead even by Roman-sourced standards. Unfortunately, few objects made of calamine brass from the Near and Middle East have been analyzed for manganese and lead, so items that might contain zinc from Jabal Dhaylan have not been identified. The calamine at Calamine Hill is present in the form of veins and irregular masses on the surface. This material could

have been extracted in limited quantities without leaving the telltale signs of mining. Metal tools would have been too valuable to leave behind, considering the remote location.

Another use of calamine was as an ingredient in eye medicine. Ophthalmia was a common eye disease in ancient times. Greek ostraca (pottery shards used for writing) from Thebes in Upper Egypt dating from the 2nd through 4th centuries CE contain the formula for an eye salve that includes calamine as a main ingredient (Lougovoya, 2020. Part 2, Medicine). In addition to calamine, the salve included acacia (gum Arabic), burnt copper, erica fruit, opium and others ingredients (Youtie, 1977). Calamine was used in medicines in Egypt as early as the 19th to 14th centuries BC (Campbell and David, 2005). The source of calamine in Egypt were small occurrences in the Eastern Desert that were mined and traded by Bedouins. Natural calamine is tan in color and resembles most ordinary sedimentary rocks. The fact that calamine was traded as early as the 19th century BC speaks to the expertise of the desert Bedouin in recognizing valuable minerals.

If galena and calamine were mined at Jabal Dhaylan as ingredients for eye medications, very little material would be required to prepare powders or batches of raw material for trade; there is enough galena and calamine present on the surface at Jabal Dhaylan that mining would not be required. Trade routes that passed close to Jabal Dhaylan provided opportunities to trade these items for other goods. The ancient port of al-Qusayr (near Al Wajh), was a major point of entry for sea traders from the Egyptian Red Sea ports of Myos Hormos and Berenike beginning in the 1st century BC (Nehmé, 2022). From the port, traders could travel to Hegra, 20 km north of present-day Al-'Ula by way of Wadi al-Hamd, or south to Medina by way of Wadi al-Qura. Land routes that originated in the Aegean and passed through Medina on the way to southern Arabia were also active at this time (Westra et al., 2022). In the 8th century, with the Arab conquest of Egypt and the Levant, Egyptian and Syrian caravan routes were established to Medina through the interior and along the coast. Most inland routes converged on the city of Qurh (al-Ma'abiyat), a few km from present-day Al-'Ula, and continued south to Medina. The coastal route from Egypt continued south to the 8th century port of al-Hawra' (Umm Lajj) and the 7th century port of al-Jar (Yanbu) before striking inland (Power, 2012, Chapter 3). This route would have included Jabal Dhaylan as a stopover, as this was the only source of water for many kilometers. Any valuable commodity mined or processed at Jabal Dhaylan would have had a ready market with travelers on their journeys to and from Qurh or Medina.

In summary, it is assumed the village was a home to miners. What they mined remains unanswered. However, if only one or two families occupied the village at a time, two minerals at Area C may have provided the means to survive: galena and calamine, either of which could be prepared as powders or sold in raw form. Considering there is no evidence for mining of either material at Jabal Dhaylan, it is concluded that one or both commodities were sold as high-value medicinal agents to passing caravans. With these two products in mind, the ruins at the village should be searched for flat grinding stones or stone mortars in which galena and/or calamine would have been ground to powder. Either type of surface would be impregnated with minute fragments of galena or secondary zinc minerals. Calamine brass was prized by the Arabs in Islamic times and even small amounts of calamine may have possessed great value. If sufficiently abundant, calamine could have been stripped from the surface at Calamine Hill without leaving obvious signs of mining. Stockpiles of mined material might be located near living quarters. Close inspection may uncover evidence of both.

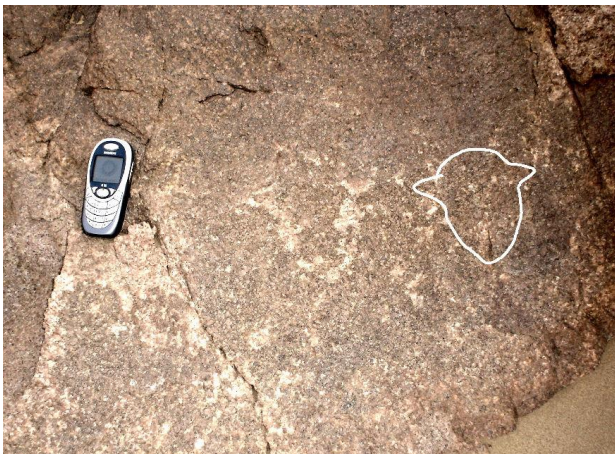


*Figure 27. Petroglyph in granite at location P3 in Figure 26. Interpreted to be the frontal profile of a sheep. Tracing offset for clarity. GPS is 10 cm long.*

#### 4.3.5 Rock Art

The location marked P3 in Fig. 26 is a petroglyph pecked into granite (Fig. 27). It is concluded that the image is the frontal profile of a sheep based on comparisons of stylized drawings of the faces of various animals such as sheep, goats, and cows. Frontal profiles of animals are exceedingly rare in the rock art of the Middle East. Of the thousands of animal petroglyphs in Google Images and Nayeem (2000), not one example could be found of a frontal profile of an animal. All representations of animals in petroglyphs are

from the side, an observation that Hodgson (2003) attributes to the way ancient people learned to record the presence of game animals. It is possible that sheep were a major source of food for the villagers and the petroglyph is a sign of reverence or affection.

## 5. SUMMARY AND CONCLUSIONS

The original purpose of this report was to simply document certain archaeological features that were encountered at Jabal Dhaylan while managing a minerals exploration program. As these features were organized, connections emerged that tied tribal symbols engraved in rocks (petroglyphs) to the local Bedouin clan, the al Jehani. It was found that the symbols could be grouped into four families, three of which still lived in the area. An archaeological study from Spain led to the discovery of the fourth family, who had travelled to al Andalus (Islamic Spain) during the Arab conquest. The evidence indicates that the al Jehani clan has lived at Jabal Dhaylan since the 7th century, but probably much longer based on the apparent age of the petroglyphs in Area A. Several of the tribal symbols of the al Jehani are also found in Al-'Ula, 300 km by land to the northeast. It is speculated that one or more of the original al Jehani families came from this area. Additional connections to Al-'Ula include symbols from early civilizations that were found with the al Jehani tribal symbols in Spain.

The presence of an ancient lithic site where high quality stone was quarried and possibly fashioned into tools indicates the Red Sea coastal route was used by early modern humans. The style of chipping appears to be Levallois, which dates the site to the Middle Paleolithic. The remains of a structure at the site may date from that time. The remnants of silver smelting at the north end of Jabal Dhaylan was dated to 3800 BC, making it one of the oldest sites in the Middle East where silver was smelted from lead ore. More recent dates indicate the site was revisited several times in the latter half of the 7th century, again in the pursuit of silver. The demonstrated lack of silver at the location, and the presence of a mining village which may date from the same period, suggests that the site was exploited for galena and calamine as ingredients for eye medications.

This study demonstrates that isolated locations may preserve the tribal symbols of family groups that would otherwise be lost in more populated areas. This makes these locations uniquely valuable for archaeologists and anthropologists attempting to establish the identity of and relationships between Arab clans or tribes.

## ACKNOWLEDGEMENTS

Dr. Abdullah A. Al-Zahrani, General Director of Archaeological Researches and Studies, Saudi Commission for Tourism and National Heritage, kindly provided permission to include the analytical data for the charcoal and crucible samples. Permission to include Fig. 20 was provided by Dr. Leonardo García Sanjuán. The author benefited from early discussions with Drs. Lloyd Weeks and Rémy Crassard. Thanks are extended to Dr. Timothy Hayes for providing reports and discussion on the Area C zinc deposits. Hugo Hemp of Marbella, Spain, provided valuable advice on Spanish literature. This study was self funded.

## REFERENCES

- Abulhab, S.D. (2017). Early Mashq and Kufic Scripts: A Historic and Typographic Introduction. In *A Handbook of Early Arabic Kufic Script: Reading, Writing, Calligraphy, Typography, Monogram*, edited by S.M.V. Mousavi Jazayeri, P.E. Michinni, and S.D. Abulhab, pp. 11-24. City University of New York (CUNY).
- Ahmed-Khalid-Abdallah, T. (2010). The Lahawiyin: Identity and History in a Sudanese Arab Tribe. PhD E-Thesis, online. Durham University. <http://ethesis.dur.ac.uk/707/>
- Akkermans, P.M.M.G. and Brüning, M.L. (2017). Nothing but cold ashes? The cairn burials of Jebel Qurma, northeastern Jordan. *Near Eastern Archaeology* 80(2), pp. 132-139. DOI: 10.5615/neareastarch.80.2.0132
- Anguilano, L., Timberlake, S. and Rehren, T. (2010). An early medieval lead-smelting bole from Banc Tynddol, Cwmystwyth, Ceredigion. *Historical Metallurgy* 44(2), pp. 85-103.
- Bailey, G. (2009). The Red Sea, coastal landscapes, and hominin dispersals. In *The Evolution of Human Populations in Arabia: Paleoenvironments, Prehistory and Genetics*, edited by M.D. Petraglia and J.I. Rose, pp. 15-39. Springer.
- Bard, K. and Fattovich, R. (2015). Egyptian long-distance trade in the Middle Kingdom and the evidence at the Red Sea harbor at Mersa/Wadi Gawasis. In *Walls of the Prince: Egyptian Interactions with Southwest Asia in Antiquity. Essays in Honour of John S. Holladay Jr.* Edited by E. B. Banning and T.P. Harrison, pp. 1-10. Leiden.
- Bednarik, R.G. (2008). Cupules. *Rock Art Research* 2008 25, pp. 61-100.
- Bednarik, R.G. and Khan, M. (2005). Scientific Studies of Saudi Arabian Rock Art. *Rock Art Research* 2005 22, pp. 49-81.
- Bednarik, R.G. and Khan, M. (2015). A chronology of Saudi Arabian rock art. In *Prospects for the Prehistoric Art Research. Proceedings of the XXVI Valcamonica Symposium, September 9 to 12, 2105*.
- Bimson, M. (1980). Cosmetic pigments from the "Royal Cemetery" at Ur. *Iraq* 42(1), pp. 75-77.
- Bisal, F. & Nielsen, K.F. (1961). Movement of soil particles in saltation. *Canadian Journal of Soil Science* 42, pp. 81-86.
- Blankinship, K.Y. (1994). *The End of the Jihād State: The Reign of Hishām ibn ‘Abd al-Malik and the Collapse of the Umayyads*. Albany, New York: State University of New York Press.
- Boivin, N. and Fuller, D.Q. (2009). Shell middens, ships and seeds: Exploring coastal subsistence, maritime trade and the dispersal of domesticates in and around the ancient Arabian Peninsula. *Journal of World Prehistory* 22, pp. 113-180. DOI: 10.1007/s10963-009-9018-2
- Bouchaud, C., Newton, C., Van Der Veen, M. and Vermeeren, C. (2018). Fuelwood and wood supplies in the Eastern Desert of Egypt during Roman times. In *The Eastern Desert of Egypt during the Greco-Roman Period: Archaeological Reports* (online). Paris. Collège de France, 2018. DOI: 10.4000/books.cdf.5237
- Bridges, N.T., Phoreman, J., White, B.R., Greeley, R., Eddlemon, E.E., Wilson, G.R., and Meyer, C.J. (2005). Trajectories and energy transfer of saltation particles onto rock surfaces: Application to abrasion and ventifact formation on Earth and Mars. *Journal of Geophysical Research* 110, E12004, pp. 1-24. DOI: 10.1029/2004JE002388
- Campbell, J. and David, A.R. (2005). Some aspects of the practice of pharmacy in ancient Egypt 1850 B.C. to 1300 B.C. *Journal of Biological Research* 1(LXXX), pp. 331-334.
- Catherine, C.J. (2005). Kohl as traditional women's adornment in North Africa and Middle East. *Introduction to Harquus: Part 2: Kohl*, pp. 1-9.
- Craddock, P.T., Freestone, I.C., Gurjar, L.K., Hegde, K.T.M., and Sonawane, V.H. (1985). Early zinc production in India. *Mining Magazine*, January, pp. 45-52.
- Craddock, P.T., La Niece, S.C. and Hook, D.R. (1998). Brass in the Medieval Islamic World. In *2000 Years of Zinc and Brass*, edited by P.T. Craddock, pp. 73-114. *British Museum Occasional Publication No. 50*.
- Craddock, P.T. (2014). Production of Silver across the Ancient World. *ISIJ International* 54, pp. 1085-1092.

- DOI: 10.2355/isijinternational.54.1085
- Crassard, R. and Hilbert, Y.H. (2013). A Nubian complex site from central Arabia: Implications for Levallois taxonomy and human dispersals during the Upper Pleistocene. *PLoS One* 8(7), E69221. DOI: 10.1371/Journal.Pone.0069221
- Crassard, R. and Petraglia, M. (2014). Stone technology of Arabia. Chapter in *Encyclopaedia of the History of Science, Technology, and Medicine in Non-Western Cultures*. Springer. DOI: 10.1007/978-94-007-3934-5\_10043-1.
- Dee, M., Wengrow, D., Shortland, A., Stevenson, A., Brock, F., Flink, L.G. and Ramsey, C.B. (2013). An absolute chronology for early Egypt using radiocarbon dating and Bayesian statistical modeling.
- Doe, B.R. and Rohrbough, R. (1977). Lead isotope data bank: 3,458 samples and analyses cited. *United States Geological Survey Open-File Report* 79-661.
- Gale, N.H. and Stos-Gale, Z.A. (1981). Ancient Egyptian Silver. *The Journal of Egyptian Archaeology* 67, pp. 103-115.
- Gilmore, M., al-Ibrahim, M., Mursi, G. and al-Talhi, D. (1985). A preliminary report on the first season of excavations at al-Mabiyat, an early Islamic site in the northern Hijaz. *Atlat* 9, pp.109-125.
- Groucutt, H.S. and Petraglia, M.D. (2012). The prehistory of the Arabian Peninsula: deserts, dispersals, and demography. *Evolutionary Anthropology* 21, pp. 113-125. DOI: 10.1002/evan21308
- Guérin, G., Mercier, N., and Adamiec, G. (2011). Dose-rate conversion factors: update. *Ancient TL* 29(1), pp. 5-8.
- Hassan, Y.F. (1967). *The Arabs and the Sudan: from the seventh to the early sixteenth century*. Edinburgh.
- Hansen, S., Montero-Ruiz, I., Rovira, S., Steiniger, D. and Toderas, M. (2019). The earliest lead ore processing in Europe. 5th millennium BC finds from Pietrele on the Lower Danube. *PLoS ONE* 14(4): e0214218. DOI: 10.1371/journal.pone.0214218.
- Hauptmann, A., Klein, S., Zettler, R., Baumer, U. and Dietemann, P. (2016). On the making and provenancing of pigments from the Early Dynastic royal tombs of Ur, Mesopotamia. *Metalla Nr.* 22(1), pp. 41-74.
- Hausleiter, A., Dinies, M., Bouchaud, C., Intilia, A., Schimmel, L. and Zur, A. (2021). Al-'Ula, Saudi-Arabia. *Archaeology and environment from the early Bronze Age (3rd mill. BCE) onwards. Season 2019*. e-Forschungsberichts des Deutschen Archäologischen Instituts, 2021(1), pp. 1-22. DOI: 10.34780/b5t2-t68
- Hay, M. (2017). Genetic history of the Spaniards and the Portuguese. *Euredia.com. Genetics*.
- Hayes, T.S., Sutley, S.J., Kadi, K.A., Balkhiyour, M.B., Siddiqui, A.A., Beshir, Z. and Hashim, H.I. (2002). Jabal Dhaylan zinc-lead deposits, geologic setting, genesis, and 1996-2000 exploration programs. Volume I-text, appendix 1 and plates. *Saudi Geological Survey, Open-File Report SGS-Of-2001-5*.
- Hayes, T.S., Sutley, S.J., Al-Shanti, M., Al-Shammari, A., Al-Fissa, A., Nadra, A. and Siddiqui, A.A. (2001). Jabal-Dhaylan district, Saudi Arabia. Salt-related carbonate-hosted zinc-lead deposits formed in the Red Sea early passive margin. In *Mineral deposits at the beginning of the 21st century*, edited by A. Piestrzynski and others, pp. 137-140. Proceedings of the Joint SGA-SEG Meeting, Krakov, Poland, 26-29 August 2001. Lisse, A.A. Balkema Publishers.
- Heck, G.W. (1999). Gold Mining in Arabia and the Rise of the Islamic State. *Journal of the Economic and Social History of the Orient* 42, pp. 364-395.
- Hilbert, Y.H., Crassard, R., Charloux, G. and Loreto, R. (2017). Nubian technology in northern Arabia: Impact on interregional variability of Middle Paleolithic industries. *Quaternary International* 435(A), pp. 77-93. DOI: 10.1016/j.quaint.2015.11.047
- Hodgkinson, A.K. and Frick, D.A. (2020). Identification of cobalt-coloured Egyptian glass objects by LA-ICP-MS: A case study from the 18th Dynasty workshops at Amarna, Egypt. *Mediterranean Archaeology and Archaeometry* 20(1), pp. 45-57. DOI: 10.5281/zenodo.3605660
- Hodgson, D. (2003). The biological foundations of upper Palaeolithic art: stimulus, percept, and representational imperatives. *Rock Art Research* 20(1), pp. 3-22.
- Khan, M. (1991). Recent rock art and epigraphic investigations in Saudi Arabia. In *Proceedings of the Seminar for Arabian Studies* 21, pp. 113-122. In *Proceedings of the Twenty Fourth Seminar for Arabian Studies held at Oxford on 24th - 26th July 1990*. Archaeopress.
- Khan, M. (2000). *Wusum - The tribal symbols of Saudi Arabia*. Bilingual (Eng./Arabic). Ministry of Education, Kingdom of Saudi Arabia.
- Khan, M. (2013). Rock Art of Saudi Arabia. *Arts* 2013 2, pp. 447-475. DOI: 10.3390/arts2040447
- Kharakwal, J.S. and Gurjar, L.K. (2006). Zinc and Brass in Archaeological Perspective. *Ancient Asia* 1, pp. 139-159. DOI: 10.5334/aa.06112

- Kennedy, D. (2011). The "Works of the Old Men" in Arabia: remote sensing in interior Arabia. *Journal of Archaeological Science* 38, pp. 3185-3203.
- Killick, D.J., Stephens, J.A. and Fenn, T.R. (2020). Geological constraints on the use of lead isotopes for provenance in archaeometallurgy. *Archaeometry*, 62(1), pp. 86-105. DOI: 10.1111/arcm.12573
- Kyle, J.R. and Price, P.E. (1986). Metallic sulphide mineralization in salt-dome cap rocks, Gulf Coast, U.S.A. *Transactions Institution of Mining Metallurgy B* 95, pp. B6-B16.
- Lougovaya, J. (2020). Greek literary ostraca revisited. In *Using Ostraca in the Ancient World: New Discoveries and Methodologies*, edited by Clementine Caputo and Julia Lougovaya, pp. 109-144. De Gruyter.
- Lovering, T.G. (1972). Jasperoid in the United States--Its characteristics, origin, and economic significance. United States Geological Survey Professional Paper 710. 176 p.
- Luening, S., Galka, M. and Vahrenholt, F. (2017). Warming and Cooling: The Medieval Climate Anomaly in Africa and Arabia. *Paleoceanography and Paleoclimatology* 32(11), pp. 1219-123. DOI: 10.1002/2017PA003237
- Macdonald, M.C.A., Al-Manaser, A. and Hidalgo-Chacón Diez, M. (2017). *The online corpus of the inscription of ancient North Arabia (OCIANA)*. Oxford.
- MacMichael, H.A. (1922). *A History of the Arabs in the Sudan and Some Account of the People who Preceded Them and of the Tribes Inhabiting Dárfūr*. Cambridge.
- Mahmood, Z.A., Zoha, S.M.S., Usmanghani, K., Hasan, M.M., Ali, O., Jahan, S., Saeed, A., Zaihd, R. and Zubair, M. (2009). Kohl (surma): retrospect and prospect. *Pakistan Journal of Pharmaceutical Sciences* 22(1), pp. 107-122.
- Mason, R.B., Farquhar, R.M. and Smith, P. (1992). Lead-isotope analyses of Islamic glazes: an exploratory approach. *Muqarnas* 9, pp. 67-71.
- Morton, V. (2019). *Brass from the past: Brass made, used and traded from prehistoric times to 1800*. Archaeopress Publishing. (e-Pdf)
- Mustafa, M. H. and Tayeh, S.N.A. (2014). Comments on Bedouin funeral rites in the writings of western travelers and explorers from the late 19th and early 20th centuries. *Mediterranean Archaeology and Archaeometry* 14(1), pp. 51-63
- Nehmé, L. (2022). Land (and maritime?) routes in and between the Egyptian and Arabian shores of the northern Red Sea in the Roman period. In *Networked spaces: The spatiality of networks in the Red Sea and Western Indian Ocean*, edited by C. Durand, J. Marchand, B. Redon and P. Schneider, pp. 513-528. MOM Éditions. Online.
- Nayeem, M.A. (2000). *The Rock Art of Arabia. Saudi Arabia, Oman, Qatar, the Emirates and Yemen*. Hyderabad Publishers.
- Ogden, J. (2000). Metals (Ancient Egyptian). In *Ancient Egyptian materials and technology*, edited by P.T. Nicholson and I. Shaw, pp. 148-176. Cambridge University Press.
- Pernicka, E., Rehren, Th. and Schmitt-Strecker, S. (1998). Late Uruk silver production by cupellation at Habuba Kabira, Thilo Rehren 8, Syria. In *Metallurgica Antiqua Der Anschnitt, Beiheft 8*, edited by Th. Rehren, A. Hauptmann and J. Muhly, pp. 123-135.
- Perry, R. and Adams, J. (1978). Desert varnish: evidence for cyclic deposition of manganese. *Nature* 276, pp. 489-491. DOI: 10.1038/276489a0.
- Ponting, M. (1999). East meets West in Post-Classical Bet She'an: The archaeometallurgy of culture change. *Journal of Archaeological Science* 26, pp. 1311-1321.
- Power, T. (2012). *The Red Sea from Byzantium to the Caliphate, AD 500-1000*. American University in Cairo Press.
- Riesmeier, M., Jennifer Keute, J., Veall, M-A., Borschneck, D., Stevenson, A., Garnett, A., Williams, A. and Ragan, M. (2022). Recipes of ancient Egyptian kohl's more diverse than previously thought. *Scientific Reports* 12, 5932. DOI: 10.1038/s41598-022-08669-0
- Rosenberg, T.M., Preusser, F., Fleitmann, D., Schwalb, A., Penkman, K., Schmid, T.W., Al-Shanti, M.A., Kadi, K. and Matter, A. (2011). Humid periods in southern Arabia: Windows of opportunity for modern human dispersal. *Geology* 39, pp. 1115-1118. DOI: 10.1130/G32281.1
- Sabir, H. (1991). Ancient mining and its impact on modern mineral exploration in Saudi Arabia. *Technical Report BRGM-TR-11-3. Ministry of Petroleum and Mineral Resources Directorate General of Mineral Resources*, Jeddah, Saudi Arabia.
- Sahin, F. (2020). A 'Kohl Box' from the Cilician plain in the frame of the analytical and archaeological evidence. *Mediterranean Archaeology and Archaeometry* 20(1), pp. 173-187. DOI: 10.5281/zenodo.3707804

- Sanjuán, L.G., Díaz-Guardamino, M., Wheatley, D.W., Barra, J-P.V., Rodríguez, J.A.L., Rogerio-Candelera, M.A., Erbez, A.J., Barker, D., Strutt, K. and Ariza, M.C. (2017). The epigraphic stela of Montoro (Córdoba): the earliest monumental script in Iberia? *Antiquity* 91, pp. 916–932. DOI: 10.15184/aqy.2017.86
- Shortland, A.J. (2006). Application of lead isotope analysis to a wide range of late bronze age Egyptian materials. *Archaeometry* 48(4), pp. 657-669.
- Smith, G.R., Smart, J.R. and Pridham, B.R. (1996). *New Arabian Studies*, Vol. 3. University of Exeter Press.
- Stos-Gale, Z.A. and Gale, N.H. (1981). Sources of galena, lead and silver in predynastic Egypt. In *Revue d'Archéométrie Actes du XXe symposium international d'archéométrie*, Paris 26-29 mars 1980, Volume III, pp.285-296. DOI: 10.3406/arsci.1981.1158.
- Swann, C.P., McGovern, P.E. and Fleming, S.J. (1989). Colorants in glasses from ancient Syro-Palestine: Specialized studies using PIXE spectrometry. *Nuclear Instruments and Methods in Physics Research B40/41*, pp. 615-619.
- Tāha, A.D. (1989). *The Muslim Conquest and Settlement of North Africa and Spain*. Routledge. London.
- Tengberg, M. (2012). Beginnings and early history of date palm garden cultivation in the Middle East. *Journal of Arid Environments* 86(1), pp. 139-147.
- Thomas, H., Kennedy, M.A., Dalton, M., McMahan, J., Boyer, D. and Repper, R. (2021). The mustatils: cult and monumentality in Neolithic north-western Arabia. *Antiquity* 2021, pp. 1-22. doi.org/10.15184/aqy.2021.51
- Thornton, C.P. and Ehlers, C.B. (2003). Early brass in the ancient Near East. *Institute for Archaeo-Metallurgical Studies* 23, pp. 3-8.
- Vermeeren, C.E. (1998). Chapter Sixteen. Wood and Charcoal. In *Berenike 1996: Report in the 1996 Excavations at Berenike (Egyptian Red Sea Coast) and the Survey of the Eastern Desert*, edited by S.E. Sidebotham and W.Z. Wendrich, pp. 331-348. Research School CNWS. Leiden.
- Weeks, L.R. (2004). An analysis of late pre-Islamic copper-base artefacts from Ed-Dur, UAE. *Arabian Archaeology and Epigraphy* 15, pp. 240-252. DOI: 10.1111/j.1600-0471.2004.00249x
- Weeks, L.R. (2012). Chapter 16. Metallurgy. In *A Companion to the Archaeology of the Ancient Near East*, edited by D.T. Potts, pp. 295-326. Blackwell Publishing Ltd.
- Westra, A.J.D, Ioannis, L., and Changhong, M. (2022). Development of the Aegean-Arabian contacts during the 1st millennium BCE: A historical and archaeological overview. *Mediterranean Archaeology and Archaeometry* 22(2), pp. 139-137. DOI: 10.5281/zenodo.6815453
- Wolf, S., Stos, S., Mason, R.B. and Tite, M. (2003). Lead-isotope analysis of Islamic pottery glazes from Fustat, Egypt. *Archaeometry* 45(3), pp. 405-420. DOI: 10.1111/1475-4754.00118
- Worthing, M.A. and Sutherland, H.H. (1996). The composition and origin of massicot, litharge (PbO), and a mixed oxide of lead used in traditional medicine in the Arabian Gulf. *Mineralogical Magazine* 60, pp. 509-513.
- Youtie, L.C. (1977). O. Bodl. II 2182 and 2185. *Bulletin of the American Society of Papyrologists* 14(1), pp. 39-43.

## Appendix I Luminescence Report

### LUMINESCENCE ANALYSIS OF CRUCIBLE FROM SAUDI ARABIA

5 September 2018

James K. Feathers  
Luminescence Dating Laboratory  
University of Washington  
Seattle, WA 98195-3412  
Email: jimf@u.washington.edu

This report presents the results of luminescence analysis of a ceramic crucible collected from Jabal Daylan, a prehistoric mining site on the Red Sea, Saudi Arabia.

The sample was submitted by Gary Clifton, geologist from Coleville, CA.

The sample was found on the surface.

Some nearby charcoal has been dated by radiocarbon to AD 600-700.

The sample was given the lab number of UW3682.

Laboratory procedures are given in the appendix.

Luminescence was measured on 1-8  $\mu\text{m}$  fine-grains.

Some coarse-grain (180-212 $\mu\text{m}$  quartz and feldspar) measurements were attempted but were abandoned because sensitivity was low

#### Dose rate

The dose rate was measured only on the ceramic.

There was no associated sediment available to estimate the external gamma dose rate.

It was assumed that the sediment had similar radioactivity as the ceramic.

This assumption is relatively safe.

The gamma dose rate amounted to only 15% of the dose rate.

Assuming a higher radioactivity for the sediment with a K content of 1%, Th content of 9 ppm and U content of 3 ppm (not unrealistic for a sandy sediment) decreases the age by only about 300 years.

The concentrations of radionuclides for the ceramic are given in Table 1.

These were mainly determined using alpha counting and flame photometry.

The beta dose rate calculated from these measurements was compared with the beta dose rate measured directly by beta counting (Table 1).

They differed at one-sigma, perhaps reflecting some disequilibrium in the U decay chain.

The beta counting results, as a more direct measure, was used for the beta dose rate in age calculation.

Moisture content was estimated as  $30\pm 20\%$  of saturated value for the ceramic sherds, reflecting the arid climate.

Cosmic dose rate was determined following Prescott and Hutton (1994).

Table 2 gives total dose rate for the sample, as calculated for TL and OSL.

*Table 1. Radionuclide concentrations*

Sample	<sup>238</sup> U (ppm)	<sup>233</sup> Th (ppm)	K (%)	Beta dose rate (Gy/ka)	
				$\beta$ -counting	$\alpha$ -counting/flame photometry
UW3682	2.18 $\pm$ 0.13	1.62 $\pm$ 0.48	1.10 $\pm$ 0.06	0.95 $\pm$ 0.11	1.26 $\pm$ 0.06

Table 2. Dose rates (Gy/ka)\*

Sample	alpha	beta	gamma	cosmic	total
OSL	0.42±0.11	0.93±0.11	0.26±0.07	0.20±0.07	1.81±0.18
TL	0.41±0.15	0.93±0.11	0.25±0.07	0.20±0.07	1.80±0.21

\* Dose rates differ for OSL, TL and IRSL due to different b-values.

Also the beta dose rate is lower than that given in Table 2 due to moisture correction.

### Equivalent Dose

Equivalent dose was measured for TL, OSL and IRSL as described in the appendix.

The TL plateau was broad (260-350°C).

There was no sensitivity change with heating.

Anomalous fading was not evident, as judged from two aliquots given identical doses but measured eight weeks apart.

OSL/IRSL was measured on 6 aliquots. Scatter was high for OSL, with two high outliers needing to be removed.

The over-dispersion of the other four was still 24%.

The IRSL signal was less scattered (no over-dispersion), but the signal was weaker (about 10 times less intense than the OSL signal) and two aliquots produced no measurable signal.

IRSL stems from feldspars, which are prone to anomalous fading.

A relatively strong IRSL signal may suggest the OSL signal partly stems from feldspars and therefore may fade, while a weak IRSL suggests the OSL is dominated by quartz.

Another measure of feldspar contribution is the size of the OSL b-value.

The b-value is a measure of alpha luminescence efficiency, and is usually less than 0.7 for quartz and a higher value for feldspar.

For these samples the OSL b-value was a little higher than the range of quartz.

As a test of the SAR procedures, a dose recovery test was performed.

The derived dose was within 2-sigma of the administered dose for OSL.

The IRSL measurement produced no meaningful result.

Equivalent dose and b-values are given in Table 3.

Table 3. Equivalent dose and b-value - fine grains

Sample	Equivalent dose (Gy)			b-value (Gy $\mu\text{m}^2$ )		
	TL	IRSL	OSL	TL	IRSL	OSL
UW3682	9.66±2.67	18.5±1.74	10.5±1.53	0.92±0.32	3.89±0.34	0.94±0.22

### Ages

The ages calculated for TL (with no correction for fading), IRSL and OSL did not differ at 2-sigma., which is another indication of insignificant fading for either TL or IRSL.

A weighted average was calculated at  $5.81 \pm 0.56$  ka, or BC  $3800 \pm 560$ .

The percent error is 9.7%.

This age is much older than the radiocarbon dates.

### Sub-Appendix 1

#### Procedures for Thermoluminescence Analysis of Pottery

##### Sample preparation -- fine grain

The sherd is broken to expose a fresh profile.

Material is drilled from the center of the cross-section, more than 2 mm from either surface, using a tungsten carbide drill tip.

The material retrieved is ground gently by an agate mortar and pestle, treated with HCl, and then settled in acetone for 2 and 20 minutes to separate the 1-8  $\mu\text{m}$  fraction.

This is settled onto a maximum of 72 stainless steel discs.

### *Glow-outs*

Thermoluminescence is measured by a Daybreak reader using a 9635Q photomultiplier with a Corning 7-59 blue filter, in N<sub>2</sub> atmosphere at 1°C/s to 450°C.

A preheat of 240°C with no hold time precedes each measurement.

Artificial irradiation is given with a <sup>241</sup>Am alpha source and a <sup>90</sup>Sr beta source, the latter calibrated against a <sup>137</sup>Cs gamma source.

Discs are stored at room temperature for at least one week after irradiation before glow out.

Data are processed by Daybreak TLApplic software.

### *Fading test*

Several discs are used to test for anomalous fading.

The natural luminescence is first measured by heating to 450°C.

The discs are then given an equal alpha irradiation and stored at room temperature for varied times: 10 min, 2 hours, 1 day, 1 week and 8 weeks.

The irradiations are staggered in time so that all of the second glows are performed on the same day.

The second glows are normalized by the natural signal and then compared to determine any loss of signal with time (on a log scale).

If the sample shows fading and the signal versus time values can be reasonably fit to a logarithmic function, an attempt is made to correct the age following procedures recommended by Huntley and Lamothe (2001).

The fading rate is calculated as the g-value, which is given in percent per decade, where decade represents a power of 10.

### *Equivalent dose*

The equivalent dose is determined by a combination additive dose and regeneration (Aitken 1985).

Additive dose involves administering incremental doses to natural material.

A growth curve plotting dose against luminescence can be extrapolated to the dose axis to estimate an equivalent dose, but for pottery this estimate is usually inaccurate because of errors in extrapolation due to nonlinearity.

Regeneration involves zeroing natural material by heating to 450°C and then rebuilding a growth curve with incremental doses.

The problem here is sensitivity change caused by the heating.

By constructing both curves, the regeneration curve can be used to define the extrapolated area and can be corrected for sensitivity change by comparing it with the additive dose curve.

This works where the shapes of the curves differ only in scale (i.e., the sensitivity change is independent of dose).

The curves are combined using the "Australian slide" method in a program developed by David Huntley of Simon Fraser University (Prescott et al. 1993).

The equivalent dose is taken as the horizontal distance between the two curves after a scale adjustment for sensitivity change.

Where the growth curves are not linear, they are fit to quadratic functions.

Dose increments (usually five) are determined so that the maximum additive dose results in a signal about three times that of the natural and the maximum regeneration dose about five times the natural.

A plateau region is determined by calculating the equivalent dose at temperature increments between 240° and 450°C and determining over which temperature range the values do not differ significantly.

This plateau region is compared with a similar one constructed for the b-value (alpha efficiency), and the overlap defines the integrated range for final analysis.

### *Alpha effectiveness*

Alpha efficiency is determined by comparing additive dose curves using alpha and beta irradiations.

The slide program is also used in this regard, taking the scale factor (which is the ratio of the two slopes) as the b-value (Aitken 1985).

### *Radioactivity*

Radioactivity is measured by alpha counting in conjunction with atomic emission for <sup>40</sup>K.

Samples for alpha counting are crushed in a mill to flour consistency, packed into plexiglass containers with ZnS:Ag screens, and sealed for one month before counting.

The pairs technique is used to separate the U and Th decay series. For atomic emission measurements, samples are dissolved in HF and other acids and analyzed by a Jenway flame photometer.

K concentrations for each sample are determined by bracketing between standards of known concentration. Conversion to  $^{40}\text{K}$  is by natural atomic abundance.

Radioactivity is also measured, as a check, by beta counting, using a Risø low level beta GM multicounter system.

About 0.5 g of crushed sample is placed on each of four plastic sample holders.

All are counted for 24 hours.

The average is converted to dose rate following Bøtter-Jensen and Mejdahl (1988) and compared with the beta dose rate calculated from the alpha counting and flame photometer results.

Both the sherd and an associated soil sample are measured for radioactivity.

Additional soil samples are analyzed where the environment is complex, and gamma contributions determined by gradients (after Aitken 1985: appendix H).

Cosmic radiation is determined after Prescott and Hutton (1994).

Radioactivity concentrations are translated into dose rates following Guérin et al. (2011).

#### *Moisture Contents*

Water absorption values for the sherds are determined by comparing the saturated and dried weights.

For temperate climates, moisture in the pottery is taken to be  $80 \pm 20$  percent of total absorption, unless otherwise indicated by the archaeologist.

Again for temperate climates, soil moisture contents are taken from typical moisture retention quantities for different textured soils (Brady 1974: 196), unless otherwise measured.

For drier climates, moisture values are determined in consultation with the archaeologist.

#### **Procedures for Optically Stimulated or Infrared Stimulated Luminescence of Fine-grained pottery.**

Optically stimulated luminescence (OSL) and infrared stimulated luminescence (IRSL) on fine-grain (1-8 $\mu\text{m}$ ) pottery samples are carried out on single aliquots following procedures adapted from Banerjee et al. (2001) and Roberts and Wintle (2001).

Equivalent dose is determined by the single-aliquot regenerative dose (SAR) method (Murray and Wintle 2000).

The SAR method measures the natural signal and the signal from a series of regeneration doses on a single aliquot.

The method uses a small test dose to monitor and correct for sensitivity changes brought about by preheating, irradiation or light stimulation.

SAR consists of the following steps: 1) preheat, 2) measurement of natural signal (OSL or IRSL), L(1), 3) test dose, 4) cut heat, 5) measurement of test dose signal, T(1), 6) regeneration dose, 7) preheat, 8) measurement of signal from regeneration, L(2), 9) test dose, 10) cut heat, 11) measurement of test dose signal, T(2), 12) repeat of steps 6 through 11 for various regeneration doses.

A growth curve is constructed from the L(i)/T(i) ratios and the equivalent dose is found by interpolation of L(1)/T(1).

Usually a zero regeneration dose and a repeated regeneration dose are employed to insure the procedure is working properly.

For fine-grained ceramics, a preheat of 240°C for 10s, a test dose of 3.1 Gy, and a cut heat of 200°C are currently being used, although these parameters may be modified from sample to sample.

The luminescence, L(i) and T(i), is measured on a Risø TL-DA-15 automated reader by a succession of two stimulations: first 100 s at 60°C of IRSL (880nm diodes), and then 100s at 125°C of OSL (470nm diodes).

Detection is through 7.5mm of Hoya U340 (ultra-violet) filters.

The two stimulations are used to construct IRSL and OSL growth curves, so that two estimations of equivalent dose are available.

Anomalous fading usually involves feldspars and only feldspars are sensitive to IRSL stimulation.

The rationale for the IRSL stimulation is to remove most of the feldspar signal, so that the subsequent OSL (post IR blue) signal is free from anomalous fading.

However, feldspar is also sensitive to blue light (470nm), and it is possible that IRSL does not remove all the feldspar signal.

Some preliminary tests in our laboratory have suggested that the OSL signal does not suffer from fading, but this may be sample specific.

The procedure is still undergoing study.

A dose recovery test is performed by first zeroing the sample by exposure to light and then administering a known dose.

The SAR protocol is then applied to see if the known dose can be obtained.

Alpha efficiency will surely differ among IRSL, OSL and TL on fine-grained materials.

It does differ between coarse-grained feldspar and quartz (Aitken 1985).

Research is currently underway in the laboratory to determine how much b-value varies according to stimulation method.

Results from several samples from different geographic locations show that OSL b-value is less variable and centers around 0.5.

IRSL b-value is more variable and is higher than that for OSL.

TL b-value tends to fall between the OSL and IRSL values.

We currently are measuring the b-value for IRSL and OSL by giving an alpha dose to aliquots whose luminescence have been drained by exposure to light.

An equivalent dose is determined by SAR using beta irradiation, and the beta/alpha equivalent dose ratio is taken as the b-value.

A high OSL b-value is indicative that feldspars might be contributing to the signal and thus subject to anomalous fading.

#### *Age and error terms*

The age and error for both OSL and TL are calculated by a laboratory constructed spreadsheet, based on Aitken (1985).

All error terms are reported at 1-sigma.

The reference age for ka determinations is 2018.

#### *References*

- Adamiec, G., and Aitken, M. J., 1998, Dose rate conversion factors: update. *Ancient TL* 16:37-50.
- Aitken, M.J., 1985, *Thermoluminescence Dating*, Academic Press, London.
- Banerjee, D., Murray, A. S., Bøtter-Jensen, L., and Lang, A., 2001, Equivalent dose estimation using a single aliquot of polymineral fine grains. *Radiation Measurements* 33:73-93.
- Bøtter-Jensen, L., and Mejdahl, V., 1988, Assessment of beta dose-rate using a GM multi-counter system. *Nuclear Tracks and Radiation Measurements* 14:187-191.
- Brady, N. C., 1974, *The Nature and Properties of Soils*, Macmillan, New York.
- Guérin, G., Mercier, N., and Adamiec, G., 2011, Dose-rate conversion factors: update. *Ancient TL* 29:5-8.
- Huntley, D.J., and Lamothe, M., 2001, Ubiquity of anomalous fading in K-feldspars, and measurement and correction for it in optical dating. *Canadian Journal of Earth Sciences* 38:1093-1106.
- Murray, A.S., and Wintle, A. G., 2000, Luminescence dating of quartz using an improved single-aliquot regenerative-dose protocol. *Radiation Measurements* 32:57-73.
- Prescott, J. R., Huntley, D. J., and Hutton, J. T., 1993, Estimation of equivalent dose in thermoluminescence dating – the *Australian slide* method. *Ancient TL* 11:1-5.
- Prescott, J. R., and Hutton, J. T., 1994, Cosmic ray contributions to dose rates for luminescence and ESR dating: large depths and long time durations. *Radiation Measurements* 23:497-500.
- Roberts, H. M., and Wintle, A. G., 2001, Equivalent dose determinations for polymineralic fine-grains using the SAR protocol: application to a Holocene sequence of the Chinese Loess Plateau. *Quaternary Science Reviews* 20:859-863.
- Taché, K., and Hart, J. P., 2013, Chronometric hygiene of radiocarbon data bases for early durable cooking technologies in northeastern North America. *American Antiquity* 78: 359-372.

## Appendix II

### Carbon-14 Report



Beta Analytic Inc.  
4985 S.W. 74 Court  
Miami, Florida 33155 USA  
PH: 305-667-5167  
FAX: 305-663-0964  
beta@radiocarbon.com  
www.radiocarbon.com

**Darden Hood**  
President

**Ronald Hatfield**  
**Christopher Patrick**  
Deputy Directors

June 20, 2017

Mr. Charles Clifton  
Western Resource Group LLC POB 146  
Minden, NV 89423 United States

RE: Radiocarbon Dating Results Dear Mr. Clifton,

Enclosed are the radiocarbon dating results for three samples recently sent to us. The report sheet contains the Conventional Radiocarbon Age (BP), the method used, material type, and applied pretreatments, any sample specific comments and, where applicable, the two-sigma calendar calibration range. The Conventional Radiocarbon ages have been corrected for total isotopic fractionation effects (natural and laboratory induced).

All results (excluding some inappropriate material types) which fall within the range of available calibration data are calibrated to calendar years (cal BC/AD) and calibrated radiocarbon years (cal BP). Calibration was calculated using one of the databases associated with the 2013 INTCAL program (cited in the references on the bottom of the calibration graph page provided for each sample.) Multiple probability ranges may appear in some cases, due to short-term variations in the atmospheric  $^{14}\text{C}$  contents at certain time periods. Looking closely at the calibration graph provided and where the BP sigma limits intercept the calibration curve will help you understand this phenomenon.

Conventional Radiocarbon Ages and sigmas are rounded to the nearest 10 years per the conventions of the 1977 International Radiocarbon Conference. When counting statistics produce sigmas lower than  $\pm 30$  years, a conservative  $\pm 30$  BP is cited for the result.

All work on these samples was performed in our laboratories in Miami under strict chain of custody and quality control under ISO/IEC 17025:2005 Testing Accreditation PJLA #59423 accreditation protocols. Sample, modern and blanks were all analyzed in the same chemistry lines by qualified professional technicians using identical reagents and counting parameters within our own particle accelerators. A quality assurance report is posted to your directory for each result.

Thank you for prepaying the analyses. As always, if you have any questions or would like to discuss the results, don't hesitate to contact us.

Sincerely ,

A digital signature of Darden Hood, written in a cursive script. Below the signature, the text "Digital signature on file" is printed in a small, black, sans-serif font.



**Beta Analytic**  
RADIOCARBON DATING  
Consistent accuracy delivered on time

DR. M.A. TAMERS and MR. D.G. HOOD  
4985 S.W. 74th Court  
Miami, Florida, USA 33155  
PH: 305-667-5167 FAX: 305-663-0964  
beta@radiocarbon.com

## REPORT OF RADIOCARBON DATING ANALYSES

Mr. Charles Clifton  
Western Resource Group LLC

Report Date: June 20, 2017  
Material Received: June 13, 2017

Sample Information and Data	Sample Code Number	Conventional Radiocarbon Age (BP) or Percent Modern Carbon (pMC) & Stable Isotopes
<b>Beta - 467134</b>	<b>Jabal 1</b>	Calendar Calibrated Results: 95.4 % Probability High Probability Density Range Method (HPD) <b>1300 +/- 30 BP</b> IRMS $\delta^{13}C$ : -25.0 o/oo
Submitter Material: Charcoal		<b>(64.4%) 660 - 730 cal AD (1290 - 1220 cal BP)</b>
Analyzed Material: Charred material		<b>(31.0%) 736 - 770 cal AD (1214 - 1180 cal BP)</b>
Pretreatment: (charred material) acid/alkali/acid		
Analysis Service: AMS-Standard delivery		
Percent Modern Carbon: 85.06 +/- 0.32 pMC		
Fraction Modern Carbon: 0.8506 +/- 0.0032		
D14C: -149.42 +/- 3.18 o/oo		
$\Delta^{14}C$ : -156.28 +/- 3.18 o/oo(1950:2017)		
Measured Radiocarbon Age: (without d13C correction): 1300 +/- 30 BP		
Calibration: BetaCal3.21: HPD method: INTCAL13		

Sample Information and Data	Sample Code Number	Conventional Radiocarbon Age (BP) or Percent Modern Carbon (pMC) & Stable Isotopes
<b>Beta - 467135</b>	<b>Jabal 2</b>	Calendar Calibrated Results: 95.4 % Probability High Probability Density Range Method (HPD) <b>1500 +/- 30 BP</b> IRMS $\delta^{13}C$ : -25.1 o/oo
Submitter Material: Charcoal		<b>(88.5%) 636 - 714 cal AD (1314 - 1236 cal BP)</b>
Analyzed Material: Charred material		<b>( 6.9%) 744 - 765 cal AD (1206 - 1185 cal BP)</b>
Pretreatment: (charred material) acid/alkali/acid		
Analysis Service: AMS-Standard delivery		
Percent Modern Carbon: 84.53 +/- 0.32 pMC		
Fraction Modern Carbon: 0.8453 +/- 0.0032		
D14C: -154.70 +/- 3.16 o/oo		
$\Delta^{14}C$ : -161.52 +/- 3.16 o/oo(1950:2017)		
Measured Radiocarbon Age: (without d13C correction): 1350 +/- 30 BP		
Calibration: BetaCal3.21: HPD method: INTCAL13		



Sample Information and Data	Sample Code Number	Conventional Radiocarbon Age (BP) or Percent Modern Carbon (pMC) & Stable Isotopes
<b>Beta - 467136</b>	<b>Jabal 3</b>	Calendar Calibrated Results: 95.4 % Probability High Probability Density Range Method (HPD) <b>1400 +/- 30 BP</b> IRMS $\delta^{13}C$ : -25.4 o/oo
Submitter Material: Charcoal		<b>(95.4%) 597 - 670 cal AD (1353 - 1280 cal BP)</b>
Analyzed Material: Charred material		
Pretreatment: (charred material) acid/alkali/acid		
Analysis Service: AMS-Standard delivery		
Percent Modern Carbon: 84.01 +/- 0.31 pMC		
Fraction Modern Carbon: 0.8401 +/- 0.0031		
D14C: -159.94 +/- 3.14 o/oo		
$\Delta^{14}C$ : -166.72 +/- 3.14 o/oo(1950:2017)		
Measured Radiocarbon Age: (without d13C correction): 1410 +/- 30 BP		
Calibration: BetaCal3.21: HPD method: INTCAL13		

Results are ISO/IEC-17025:2005 accredited. No sub-contracting or student labor was used in the analyses. All work was done at Beta in 4 in-house NEC accelerator mass spectrometers and 4 Thermo IRMSs. The "Conventional Radiocarbon Age" was calculated using the Libby half-life (5568 years), is corrected for total isotopic fraction and was used for calendar calibration where applicable. The Age is rounded to the nearest 10 years and is reported as radiocarbon years before present (BP), "present" = AD 1950. Results greater than the modern reference are reported as percent modern carbon (pMC). The modern reference standard was 95% the  $^{14}C$  signature of NIST SRM-4990C (oxalic acid). Quoted errors are 1 sigma counting statistics. Calculated sigmas less than 30 BP on the Conventional Radiocarbon Age are conservatively rounded up to 30.  $\delta^{13}C$  values are on the material itself (not the AMS  $\delta^{13}C$ ).  $\delta^{13}C$  and  $\delta^{15}N$  values are relative to VPDB-1. References for calendar calibrations are cited at the bottom of calibration graph pages.



BetaCal 3.21  
**Calibration of Radiocarbon Age to Calendar Years**  
 (High Probability Density Range Method (HPD): INTCAL13)

(Variables:  $\delta^{13}\text{C} = -25.1$  o/oo)

**Laboratory number**      **Beta-467135**

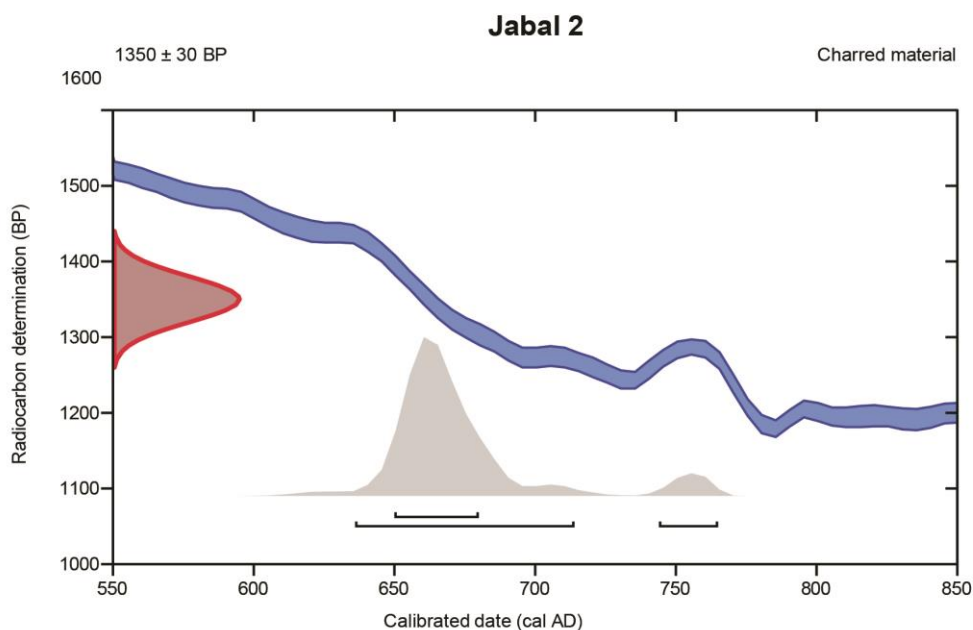
**Conventional radiocarbon age**      **1350  $\pm$  30 BP**

95.4% probability

(88.5%)	636 - 714 cal AD	(1314 - 1236 cal BP)
(6.9%)	744 - 765 cal AD	(1206 - 1185 cal BP)

68.2% probability

(68.2%)	650 - 680 cal AD	(1300 - 1270 cal BP)
---------	------------------	----------------------



#### Database used

INTCAL13

#### References

##### References to Probability Method

Bronk Ramsey, C. (2009). Bayesian analysis of radiocarbon dates. *Radiocarbon*, 51(1), 337-360.

##### References to Database INTCAL13

Reimer, et.al., 2013, *Radiocarbon*55(4).

#### Beta Analytic Radiocarbon Dating Laboratory

4985 S.W. 74th Court, Miami, Florida 33155 • Tel: (305)667-5167 • Fax: (305)663-0964 • Email: beta@radiocarbon.com





**BETA**  
Radiocarbon Dating  
*Consistent Accuracy  
Delivered On-Time*

**Beta Analytic Inc.**  
4985 SW 74 Court  
Miami, Florida 33155 USA  
Tel: 305-667-5167  
Fax: 305-663-0964  
info@betalabservices.com  
www.betalabservices.com

**Mr. Darden Hood**  
President

**Mr. Ronald Hatfield**  
**Mr. Christopher Patrick**  
Deputy Directors

*The Radiocarbon Laboratory Accredited to ISO/IEC 17025:2005 Testing Accreditation PJLA #59423*

### Quality Assurance Report

This report provides the results of reference materials used to validate radiocarbon analyses prior to reporting. Known-value reference materials were analyzed quasi-simultaneously with the unknowns. Results are reported as expected values vs measured values. Reported values are calculated relative to NIST SRM-4990B and corrected for isotopic fractionation. Results are reported using the direct analytical measure percent modern carbon (pMC) with one relative standard deviation. Agreement between expected and measured values is taken as being within 2 sigma agreement (error x 2) to account for total laboratory error.

**Report Date:** June 20, 2017  
**Submitter:** Mr. Charles Clifton

#### QA MEASUREMENTS

##### Reference 1

Expected Value: 129.41 +/- 0.06 pMC

Measured Value: 129.23 +/- 0.37 pMC

Agreement: Accepted

##### Reference 2

Expected Value: 0.44 +/- 0.10 pMC

Measured Value: 0.41 +/- 0.04 pMC

Agreement: Accepted

##### Reference 3

Expected Value: 96.69 +/- 0.50 pMC

Measured Value: 97.07 +/- 0.30 pMC

Agreement: Accepted

**COMMENT:** All measurements passed acceptance tests.

**Validation:**



**Date:** June 20, 2017